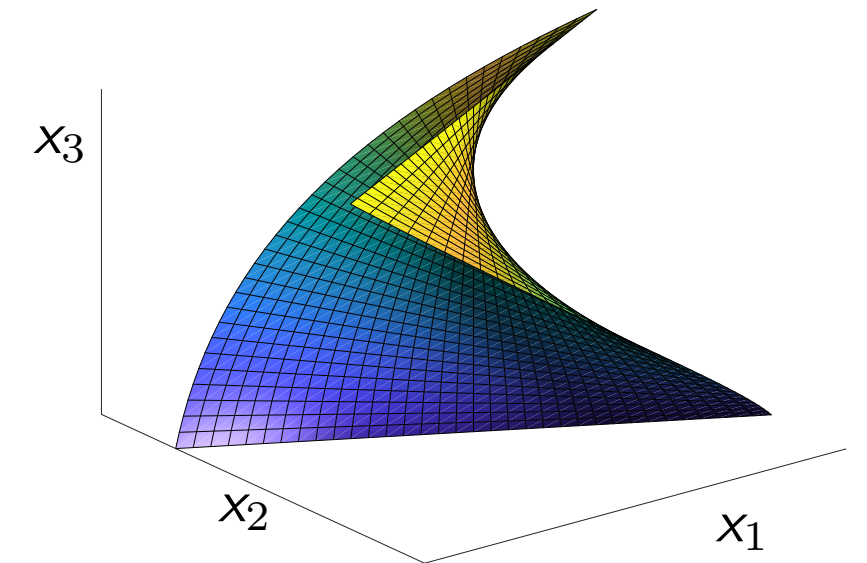
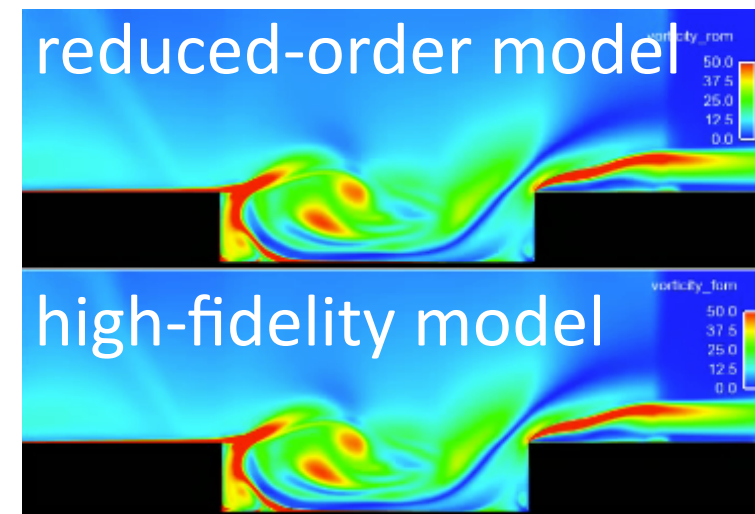
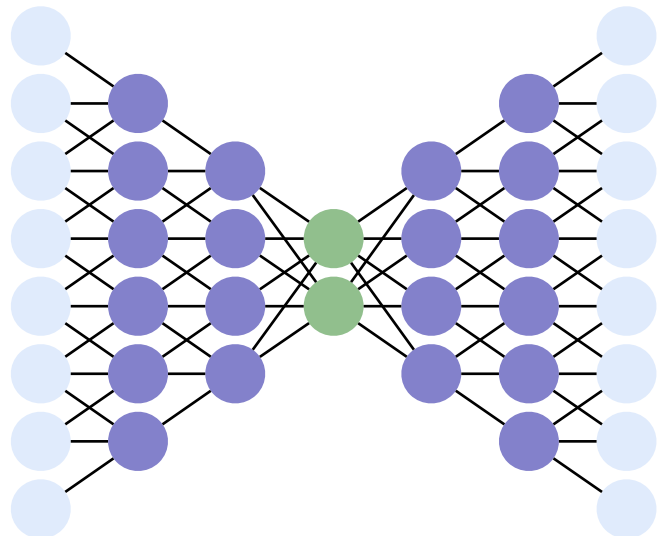


Model reduction of dynamical systems on nonlinear manifolds using deep convolutional autoencoders



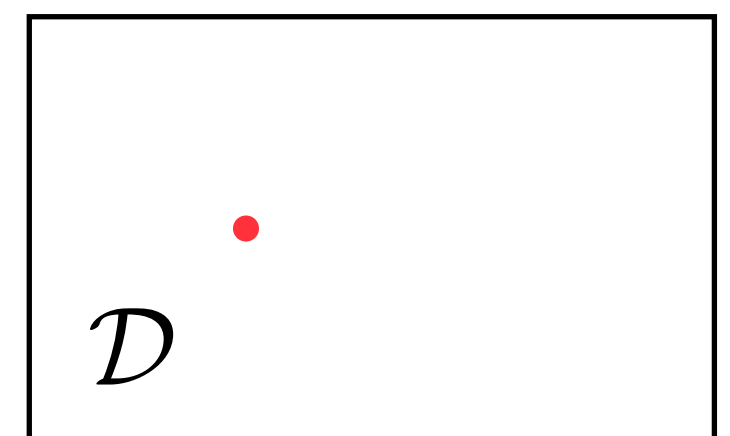
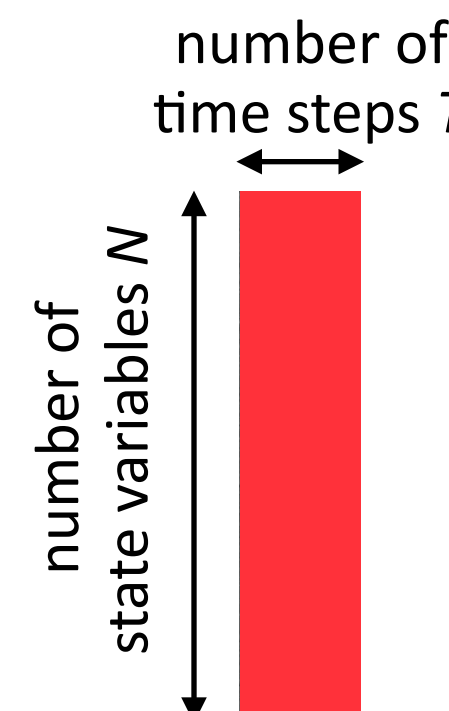
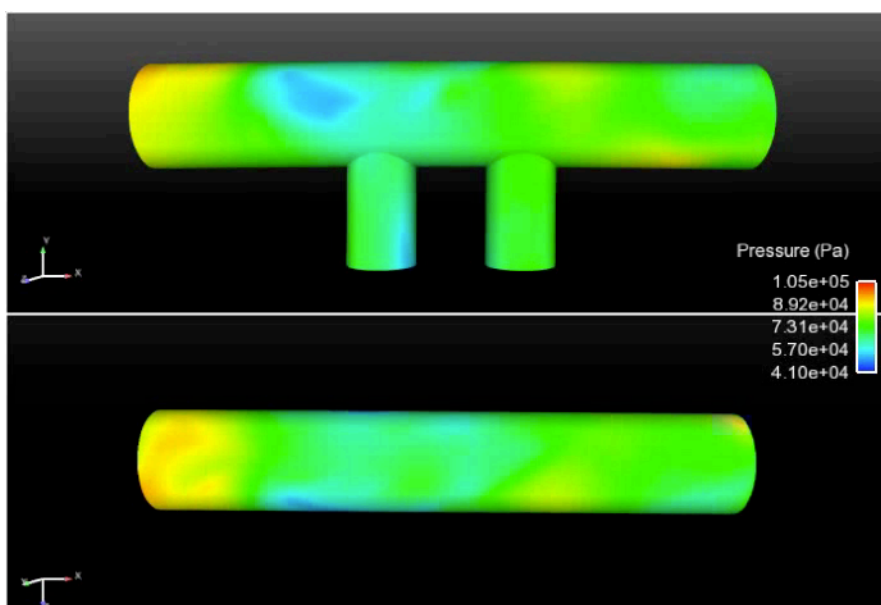
Kookjin Lee and Kevin Carlberg
Sandia National Laboratories
USNCCM
June 29, 2019

1. *Training*: Solve ODE for $\mu \in \mathcal{D}_{\text{training}}$ and collect simulation data

2. *Machine learning*: Identify structure in data

3. *Reduction*: Reduce the cost of solving ODE for $\mu \in \mathcal{D}_{\text{query}} \setminus \mathcal{D}_{\text{training}}$

$$\text{ODE: } \frac{d\mathbf{x}}{dt} = \mathbf{f}(\mathbf{x}; t, \mu)$$

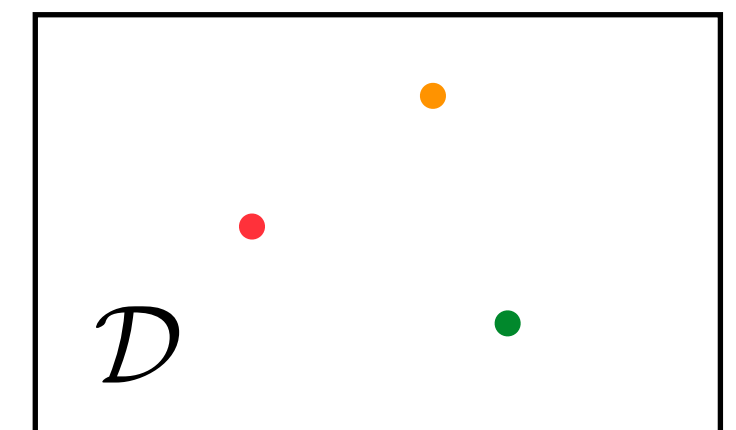
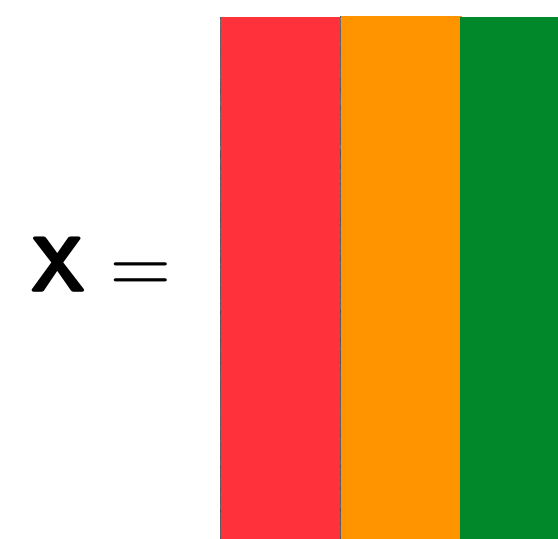
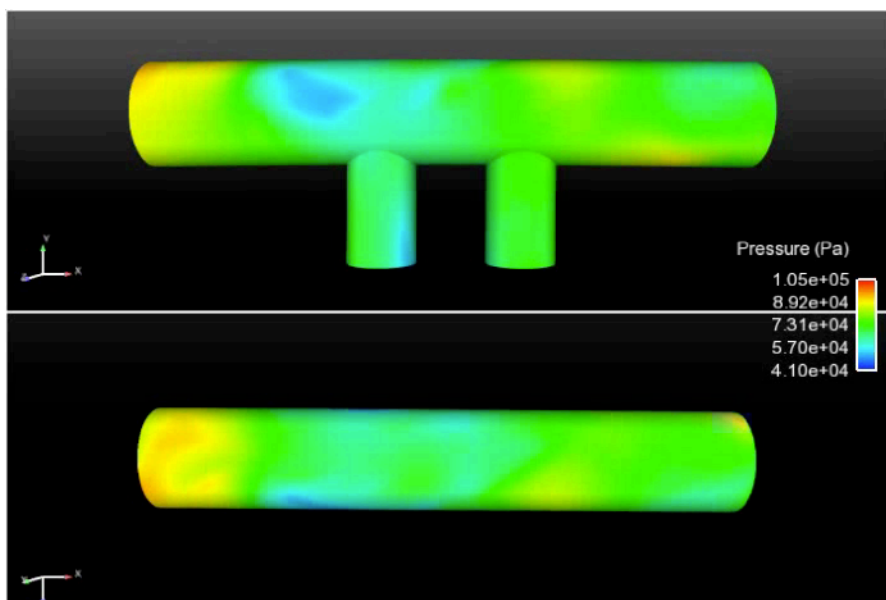


1. *Training*: Solve ODE for $\mu \in \mathcal{D}_{\text{training}}$ and collect simulation data

2. *Machine learning*: Identify structure in data

3. *Reduction*: Reduce the cost of solving ODE for $\mu \in \mathcal{D}_{\text{query}} \setminus \mathcal{D}_{\text{training}}$

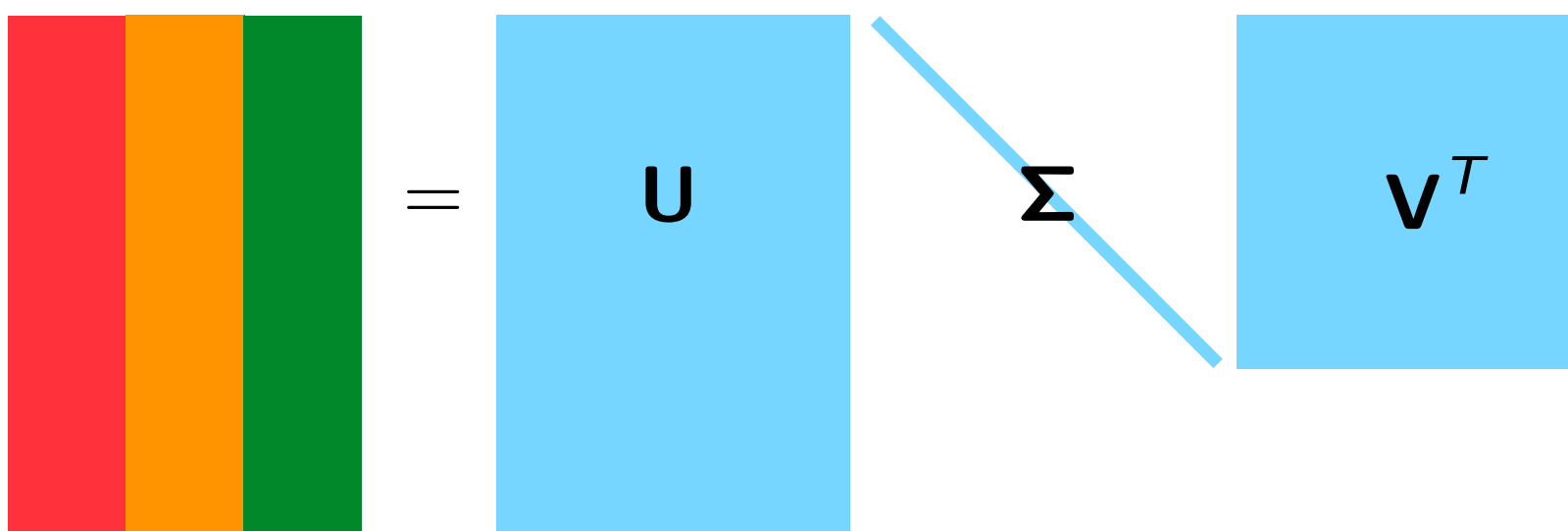
$$\text{ODE: } \frac{d\mathbf{x}}{dt} = \mathbf{f}(\mathbf{x}; t, \mu)$$



1. *Training*: Solve ODE for $\mu \in \mathcal{D}_{\text{training}}$ and collect simulation data

2. *Machine learning*: Identify structure in data

3. *Reduction*: Reduce the cost of solving ODE for $\mu \in \mathcal{D}_{\text{query}} \setminus \mathcal{D}_{\text{training}}$

$$\mathbf{X} = \begin{array}{|c|c|c|}\hline \textcolor{red}{\mathbf{X}} & \textcolor{orange}{=} & \textcolor{green}{\mathbf{U}} \\ \hline \end{array} = \mathbf{U} \Sigma \mathbf{V}^T$$


1. *Training*: Solve ODE for $\mu \in \mathcal{D}_{\text{training}}$ and collect simulation data

2. *Machine learning*: Identify structure in data

3. *Reduction*: Reduce the cost of solving ODE for $\mu \in \mathcal{D}_{\text{query}} \setminus \mathcal{D}_{\text{training}}$

$$\mathbf{X} = \begin{array}{|c|c|c|}\hline \textcolor{red}{\text{X}} & \textcolor{orange}{\text{=}} & \textcolor{green}{\text{X}} \\ \hline \end{array} = \begin{array}{|c|c|c|}\hline \Phi & \textcolor{brown}{\text{U}} & \textcolor{blue}{\Sigma} \\ \hline \end{array} \textcolor{blue}{\text{v}^T}$$

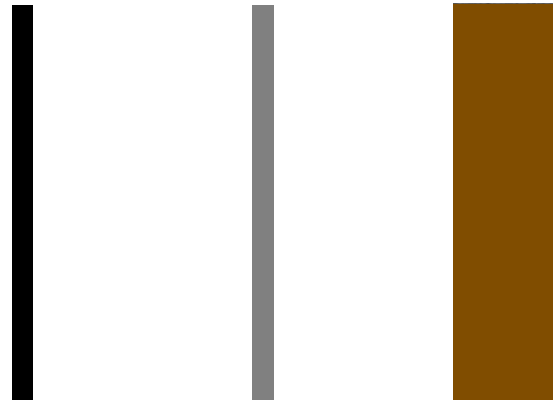
Φ columns are principal components of the spatial simulation data

1. *Training*: Solve ODE for $\mu \in \mathcal{D}_{\text{training}}$ and collect simulation data

2. *Machine learning*: Identify structure in data

3. *Reduction*: Reduce the cost of solving ODE for $\mu \in \mathcal{D}_{\text{query}} \setminus \mathcal{D}_{\text{training}}$

$$\mathbf{x}(t) \approx \tilde{\mathbf{x}}(t) = \Phi \hat{\mathbf{x}}(t)$$



ODE

$$\frac{d\mathbf{x}}{dt} = \mathbf{f}(\mathbf{x}; t) \xrightarrow[\text{minimization}]{\text{residual}}$$

$$\mathbf{r}\left(\frac{d\mathbf{x}}{dt}, \mathbf{x}, t\right) = 0$$

Galerkin ODE

$$\frac{d\hat{\mathbf{x}}}{dt} = \Phi^T \mathbf{f}(\Phi \hat{\mathbf{x}}, t)$$

$$\Phi \frac{d\hat{\mathbf{x}}}{dt} (\Phi \hat{\mathbf{x}}, t) = \arg \min_{\mathbf{v} \in \text{range}(\Phi)} \|\mathbf{r}(\mathbf{v}, \Phi \hat{\mathbf{x}}, t)\|_2$$

*time
discretization*

*time
discretization*

LSPG OΔE

[C., Bou-Mosleh, Farhat, 2011]

$$\Phi \hat{\mathbf{x}}^n = \arg \min_{\mathbf{v} \in \text{range}(\Phi)} \|\mathbf{r}^n(\mathbf{v})\|_2 \quad n = 1, \dots, T$$

*residual
minimization*

OΔE

$$\mathbf{r}^n(\mathbf{x}^n) = 0 \quad n = 1, \dots, T$$

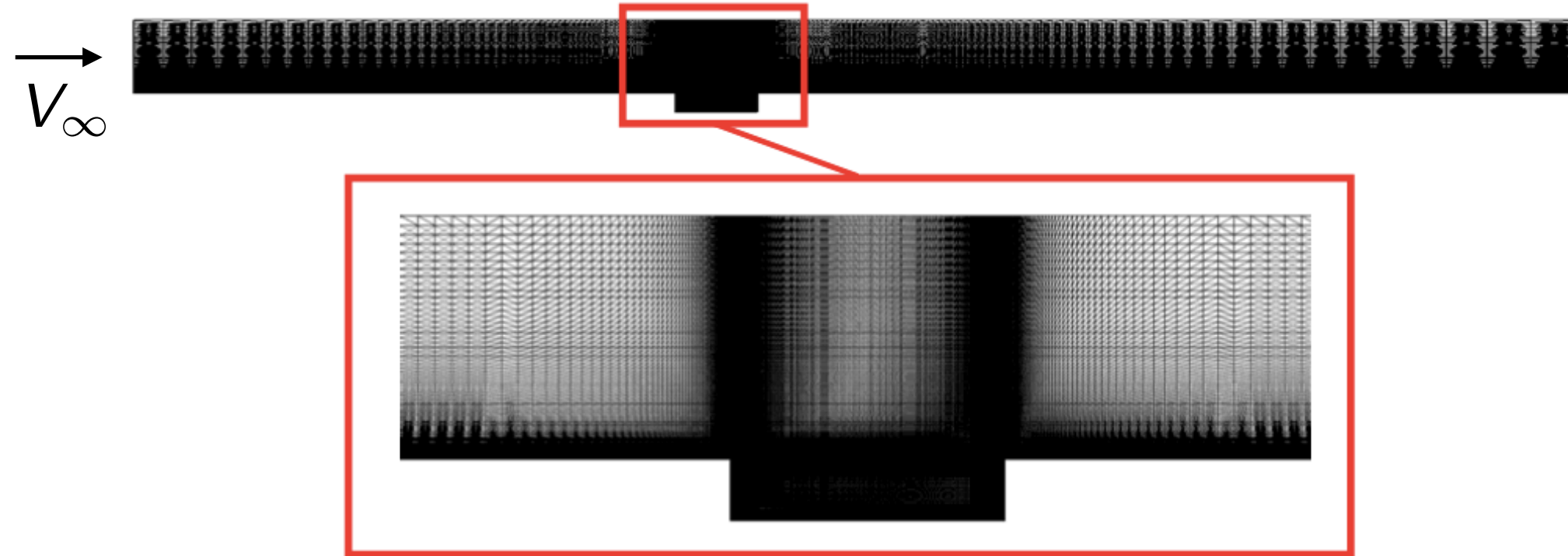
Galerkin OΔE

$$\Phi^T \mathbf{r}^n(\Phi \hat{\mathbf{x}}^n) = 0 \quad n = 1, \dots, T$$

• ODE residual: $\mathbf{r}(\mathbf{v}, \mathbf{x}, t) := \mathbf{v} - \mathbf{f}(\mathbf{x}, t)$

• OΔE residual: $\mathbf{r}^n(\mathbf{w}) := \alpha_0 \mathbf{w} - \Delta t \beta_0 \mathbf{f}(\mathbf{w}, t^n) + \sum_{j=1}^k \alpha_j \mathbf{x}^{n-j} - \Delta t \sum_{j=1}^k \beta_j \mathbf{f}(\mathbf{x}^{n-j}, t^{n-j})$

Captive carry



- Unsteady Navier–Stokes
- $\text{Re} = 6.3 \times 10^6$
- $M_\infty = 0.6$

Spatial discretization

- 2nd-order finite volume
- DES turbulence model
- 1.2×10^6 degrees of freedom

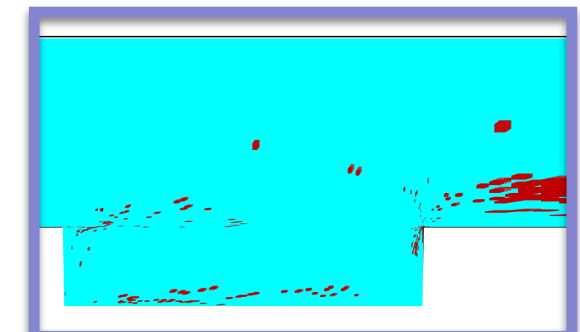
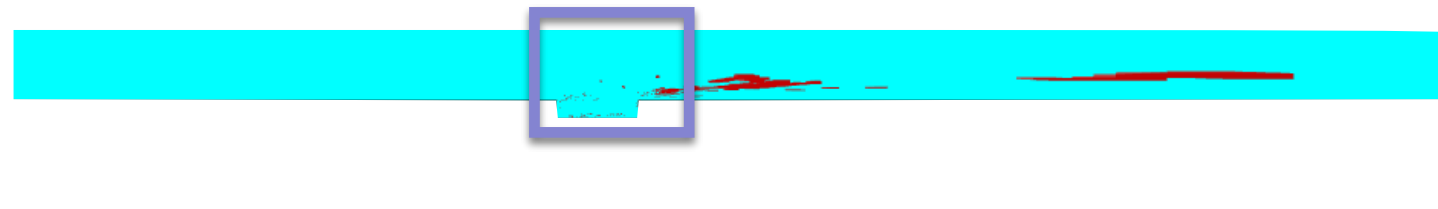
Temporal discretization

- 2nd-order BDF
- Verified time step $\Delta t = 1.5 \times 10^{-3}$
- 8.3×10^3 time instances

LSPG ROM with sample mesh [C., Barone, Antil, 2017]

$$\hat{\Phi} \mathbf{x}^n = \arg \min_{\mathbf{v} \in \text{range}(\Phi)} \|\mathbf{r}^n(\mathbf{v})\|_\Theta$$

sample
mesh

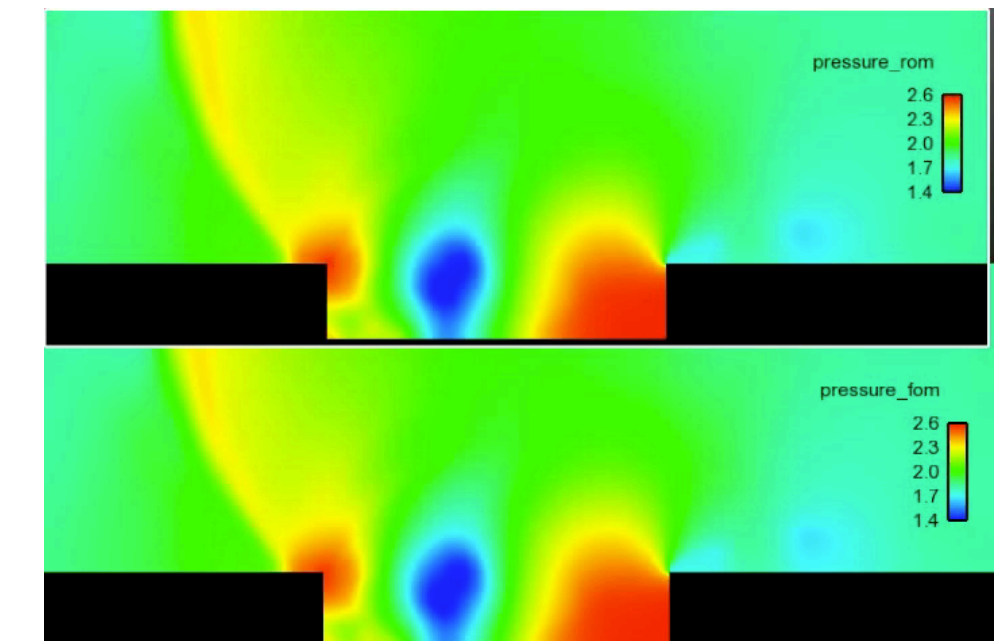
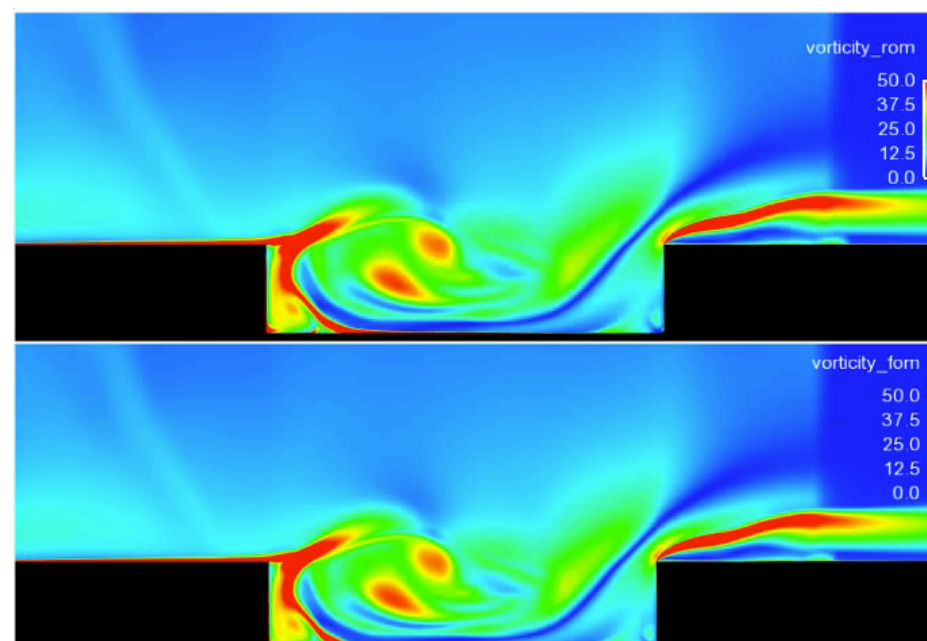


+ HPC on a laptop

vorticity field

pressure field

LSPG ROM
32 min, 2 cores

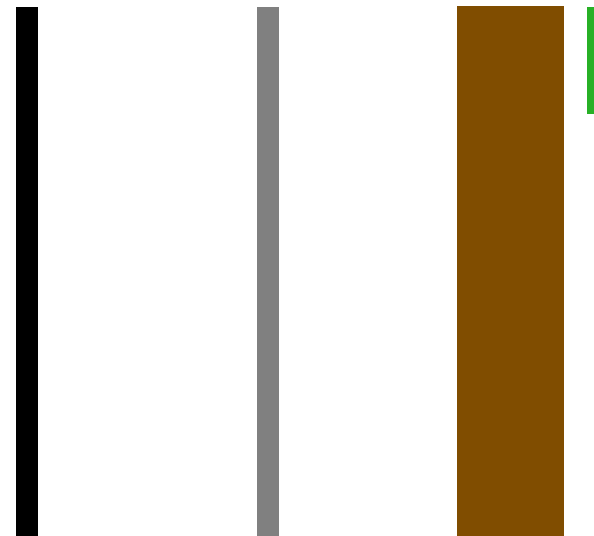


high-fidelity
5 hours, 48 cores

+ 229x savings in core-hours
+ < 1% error in time-averaged drag
... so why doesn't everyone use ROMs?

Good generalization performance is not guaranteed

$$\mathbf{x}(t) \approx \tilde{\mathbf{x}}(t) = \Phi \hat{\mathbf{x}}(t)$$



1) Linear-subspace assumption is strong ← *This talk*

- Lee and C. “Model reduction of dynamical systems on nonlinear manifolds using deep convolutional autoencoders,” arXiv e-Print, 1812.08373 (2018).

2) Accuracy limited by training data used to construct Φ

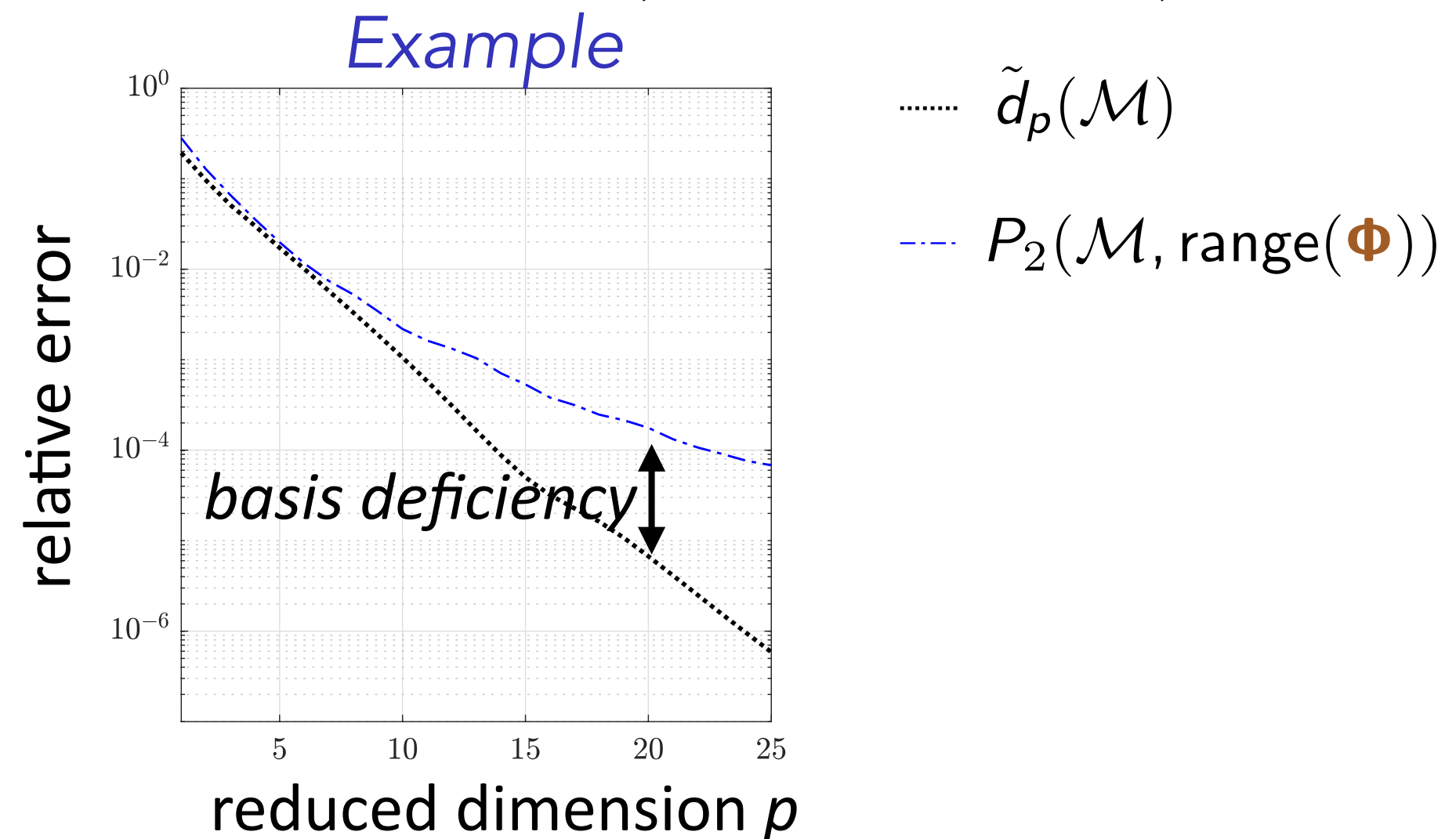
- Etter and C. “Online adaptive basis refinement and compression for reduced-order models,” arXiv e-Print, 1902.10659 (2019).
- C. “Adaptive h-refinement for reduced-order models,” Int J Numer Meth Eng, 102(5):1192–1210, 2015.

Kolmogorov-width limitation of linear subspaces

- $\mathcal{M} := \{\mathbf{x}(t, \mu) \mid t \in [0, T_{\text{final}}], \mu \in \mathcal{D}\}$: solution manifold

- \mathcal{S}_p : set of all p -dimensional linear subspaces

- $\tilde{d}_p(\mathcal{M}) := \inf_{\mathcal{S} \in \mathcal{S}_p} P_2(\mathcal{M}, \mathcal{S})$, $P_2(\mathcal{M}, \mathcal{S}) := \sqrt{\sum_{\mathbf{x} \in \mathcal{M}} \inf_{\mathbf{y} \in \mathcal{S}} \|\mathbf{x} - \mathbf{y}\|^2} / \sqrt{\sum_{\mathbf{x} \in \mathcal{M}} \|\mathbf{x}\|^2}$

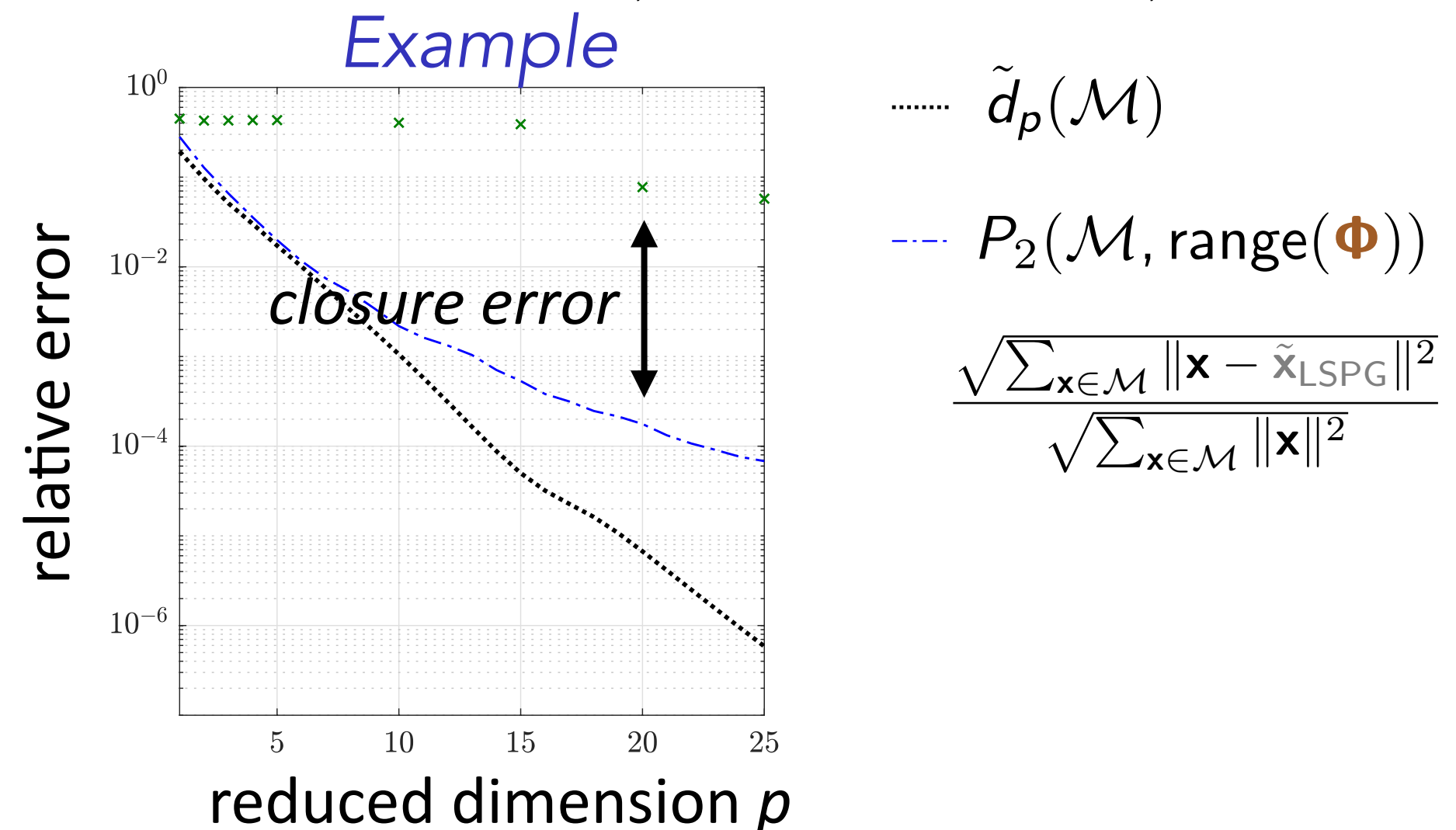


Kolmogorov-width limitation of linear subspaces

• $\mathcal{M} := \{\mathbf{x}(t, \mu) \mid t \in [0, T_{\text{final}}], \mu \in \mathcal{D}\}$: solution manifold

• \mathcal{S}_p : set of all p -dimensional linear subspaces

• $\tilde{d}_p(\mathcal{M}) := \inf_{\mathcal{S} \in \mathcal{S}_p} P_2(\mathcal{M}, \mathcal{S})$, $P_2(\mathcal{M}, \mathcal{S}) := \sqrt{\sum_{\mathbf{x} \in \mathcal{M}} \inf_{\mathbf{y} \in \mathcal{S}} \|\mathbf{x} - \mathbf{y}\|^2} / \sqrt{\sum_{\mathbf{x} \in \mathcal{M}} \|\mathbf{x}\|^2}$

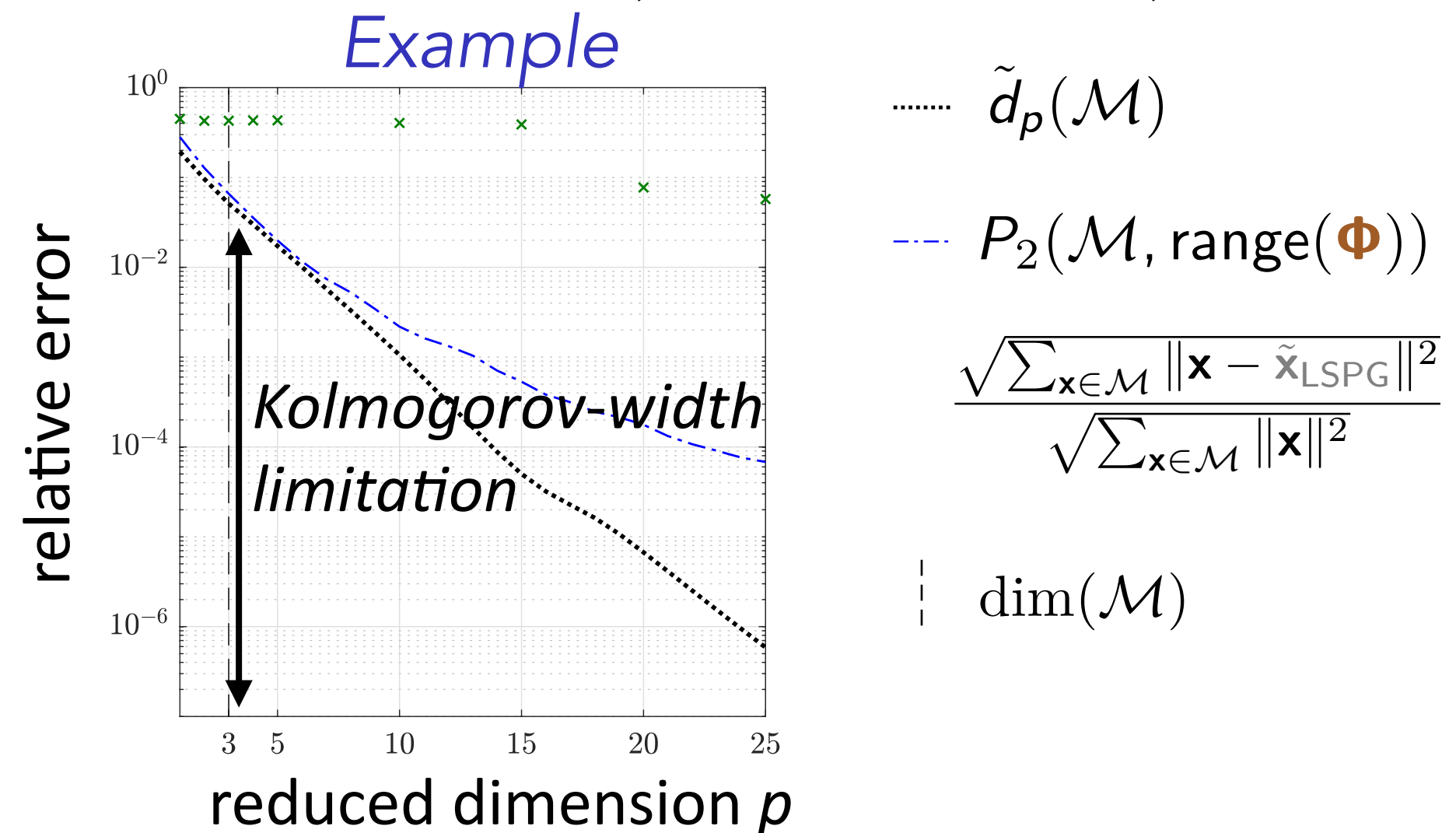


Kolmogorov-width limitation of linear subspaces

- $\mathcal{M} := \{\mathbf{x}(t, \mu) \mid t \in [0, T_{\text{final}}], \mu \in \mathcal{D}\}$: solution manifold

- \mathcal{S}_p : set of all p -dimensional linear subspaces

- $\tilde{d}_p(\mathcal{M}) := \inf_{\mathcal{S} \in \mathcal{S}_p} P_2(\mathcal{M}, \mathcal{S})$, $P_2(\mathcal{M}, \mathcal{S}) := \sqrt{\sum_{\mathbf{x} \in \mathcal{M}} \inf_{\mathbf{y} \in \mathcal{S}} \|\mathbf{x} - \mathbf{y}\|^2} / \sqrt{\sum_{\mathbf{x} \in \mathcal{M}} \|\mathbf{x}\|^2}$



- Kolmogorov-width limitation: **significant error** for $p = \dim(\mathcal{M})$

Goal: overcome limitation via projection onto a nonlinear manifold

Overcoming Kolmogorov-width limitation

Transform/update the linear subspace

[Ohlberger and Rave, 2013; Iollo and Lombardi, 2014; Gerbeau and Lombardi, 2014; Peherstorfer and Willcox, 2015; Welper, 2017; Mojgani and Balajewicz, 2017; Reiss et al., 2018; Zimmermann et al., 2018; Peherstorfer, 2018; Rim and Mandli, 2018; Rim and Mandli, 2018; Nair and Balajewicz, 2019; Cagniart et al., 2019]

- + Can work much better than a fixed basis
- Some require **problem-specific knowledge or characteristics**
- Do not consider manifolds of **general nonlinear structure**

A priori construction of local linear subspaces

[Dihlmann et al., 2011; Drohmann et al., 2011; Amsallem, Zahr, Farhat, 2012; Peherstorfer et el., 2014; Taddei et al., 2015]

- + Tailored bases for local regions of time/spatial domain, state space
- Do not consider manifolds of **general nonlinear structure**

Model reduction on nonlinear manifolds [Gu, 2011; Kashima, 2016; Hartman and Mestha, 2017]

- **Kinematically inconsistent** [Kashima, 2016; Hartman and Mestha, 2017]
- **Limited** to piecewise linear manifolds [Gu, 2011]
- **Solutions lack optimality** [Gu, 2011; Kashima, 2016; Hartman and Mestha, 2017]

Overcome shortcomings of existing methods

- + Enable manifolds with general nonlinear structure
- + Kinematically consistent
- + Satisfy optimality property

Manifold Galerkin and LSPG projection

Practical nonlinear-manifold construction

- + No problem-specific knowledge required
- + Use same snapshot data as POD

Deep convolutional autoencoders

Overcome shortcomings of existing methods

- + Enable manifolds with general nonlinear structure
- + Kinematically consistent
- + Satisfy optimality property

Manifold Galerkin and LSPG projection

Practical nonlinear-manifold construction

- + No problem-specific knowledge required
- + Use same snapshot data as POD

Deep convolutional autoencoders

Nonlinear trial manifold

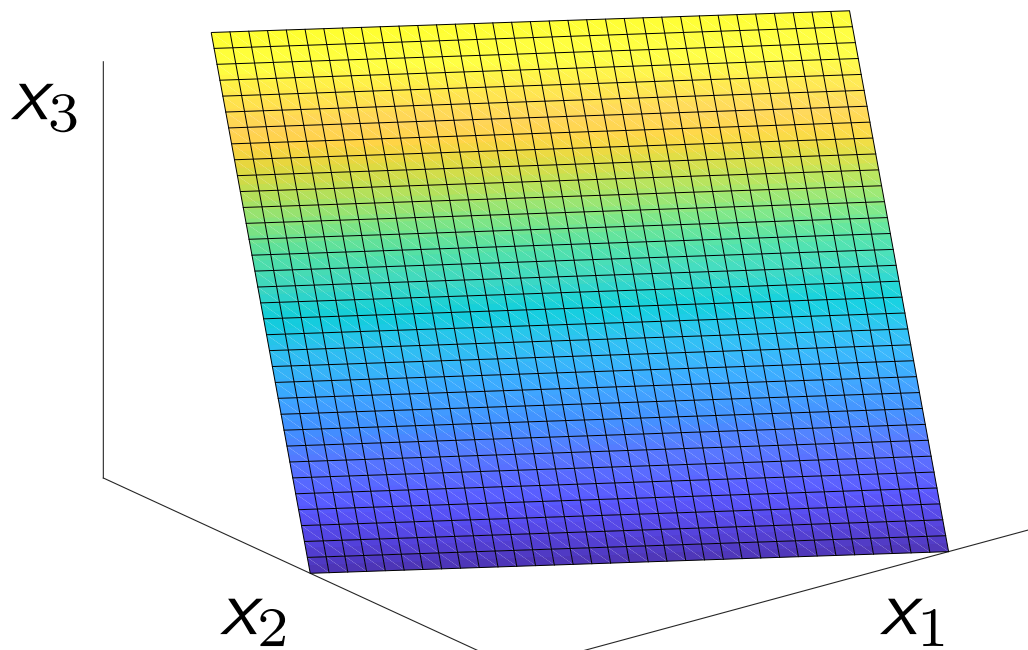
Linear trial subspace

$$\text{range}(\Phi) := \{\Phi \hat{\mathbf{x}} \mid \hat{\mathbf{x}} \in \mathbb{R}^p\}$$

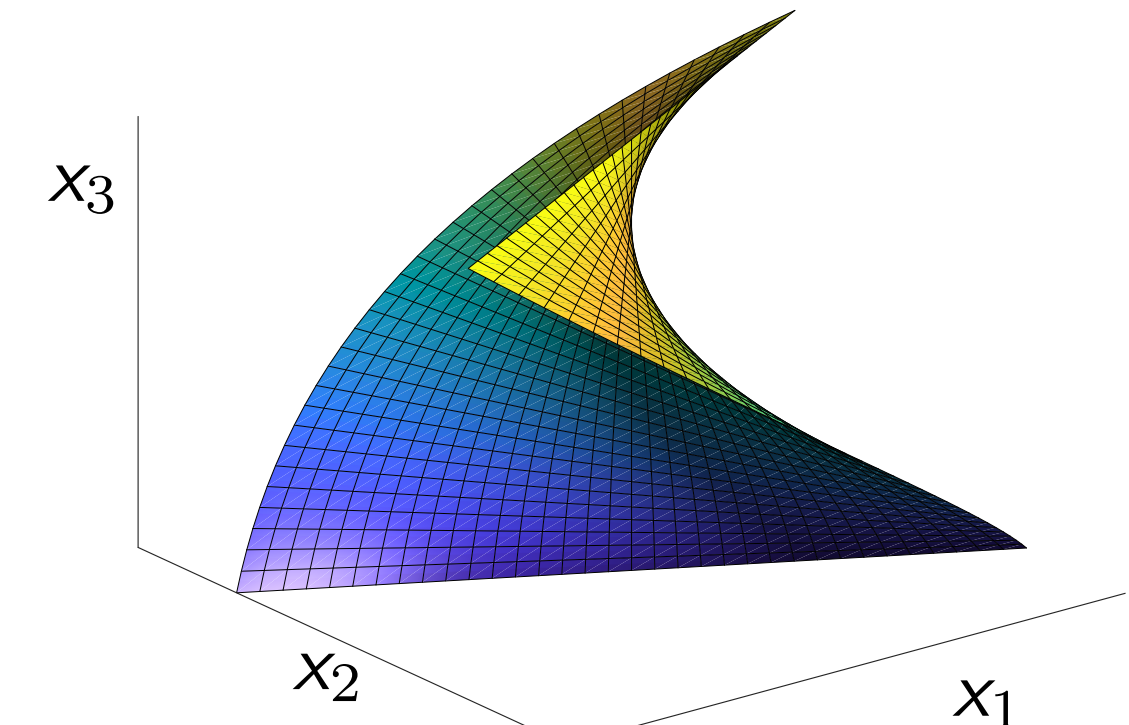
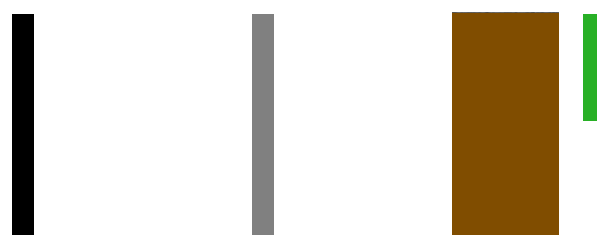
Nonlinear trial manifold

$$\mathcal{S} := \{\mathbf{g}(\hat{\mathbf{x}}) \mid \hat{\mathbf{x}} \in \mathbb{R}^p\}$$

example
 $N=3$
 $p=2$



state $\mathbf{x}(t) \approx \tilde{\mathbf{x}}(t) = \Phi \hat{\mathbf{x}}(t) \in \text{range}(\Phi)$



state $\mathbf{x}(t) \approx \tilde{\mathbf{x}}(t) = \mathbf{g}(\hat{\mathbf{x}}(t)) \in \mathcal{S}$



+ manifold has general structure

velocity $\frac{d\mathbf{x}}{dt} \approx \frac{d\tilde{\mathbf{x}}}{dt} = \Phi \frac{d\hat{\mathbf{x}}}{dt} \in \text{range}(\Phi)$

$\frac{d\mathbf{x}}{dt} \approx \frac{d\tilde{\mathbf{x}}}{dt} = \nabla \mathbf{g}(\hat{\mathbf{x}}) \frac{d\hat{\mathbf{x}}}{dt} \in T_{\hat{\mathbf{x}}} \mathcal{S}$

+ kinematically consistent

1. *Training*: Solve ODE for $\mu \in \mathcal{D}_{\text{training}}$ and collect simulation data

2. *Machine learning*: Identify structure in data

3. *Reduction*: Reduce the cost of solving ODE for $\mu \in \mathcal{D}_{\text{query}} \setminus \mathcal{D}_{\text{training}}$

Subspace ROM

Given Φ

Galerkin

$$\frac{d\hat{\mathbf{x}}}{dt} = \underset{\hat{\mathbf{v}} \in \mathbb{R}^p}{\operatorname{argmin}} \|\mathbf{r}(\Phi\hat{\mathbf{v}}, \Phi\hat{\mathbf{x}}; t)\|_2$$

\Updownarrow

$$\frac{d\hat{\mathbf{x}}}{dt} = \Phi^T \mathbf{f}(\Phi\hat{\mathbf{x}}; t)$$

LSPG

$$\hat{\mathbf{x}}^n = \underset{\hat{\mathbf{v}} \in \mathbb{R}^p}{\operatorname{argmin}} \|\mathbf{r}^n(\Phi\hat{\mathbf{v}})\|_2$$

Manifold ROM

Given $\mathbf{g}(\hat{\mathbf{x}})$

$$\frac{d\hat{\mathbf{x}}}{dt} = \underset{\hat{\mathbf{v}} \in \mathbb{R}^p}{\operatorname{argmin}} \|\mathbf{r}(\nabla \mathbf{g}(\hat{\mathbf{x}})\hat{\mathbf{v}}, \mathbf{g}(\hat{\mathbf{x}}); t)\|_2$$

\Updownarrow

$$\frac{d\hat{\mathbf{x}}}{dt} = \nabla \mathbf{g}(\hat{\mathbf{x}})^+ \mathbf{f}(\mathbf{g}(\hat{\mathbf{x}}); t)$$

- + Satisfy residual minimization

Theorem

If the following conditions hold:

1. $f(\cdot; t)$ is Lipschitz continuous with Lipschitz constant κ
2. Δt is small enough such that $0 < h := |\alpha_0| - |\beta_0|\kappa\Delta t$, then

$$\|\mathbf{x}^n - \mathbf{g}(\hat{\mathbf{x}}_G^n)\|_2 \leq \frac{1}{h} \|\mathbf{r}_G^n(\mathbf{g}(\hat{\mathbf{x}}_G))\|_2 + \frac{1}{h} \sum_{\ell=1}^k |\gamma_\ell| \|\mathbf{x}^{n-\ell} - \mathbf{g}(\hat{\mathbf{x}}_G)\|_2$$

$$\|\mathbf{x}^n - \mathbf{g}(\hat{\mathbf{x}}_{LSPG}^n)\|_2 \leq \frac{1}{h} \min_{\hat{\mathbf{v}}} \|\mathbf{r}_{LSPG}^n(\mathbf{g}(\hat{\mathbf{v}}))\|_2 + \frac{1}{h} \sum_{\ell=1}^k |\gamma_\ell| \|\mathbf{x}^{n-\ell} - \mathbf{g}(\hat{\mathbf{x}}_{LSPG})\|_2$$

+ Manifold LSPG sequentially *minimizes the error bound*

Overcome shortcomings of existing methods

- + Enable manifolds with general nonlinear structure
- + Kinematically consistent
- + Satisfy optimality property

Manifold Galerkin and LSPG projection

Practical nonlinear-manifold construction

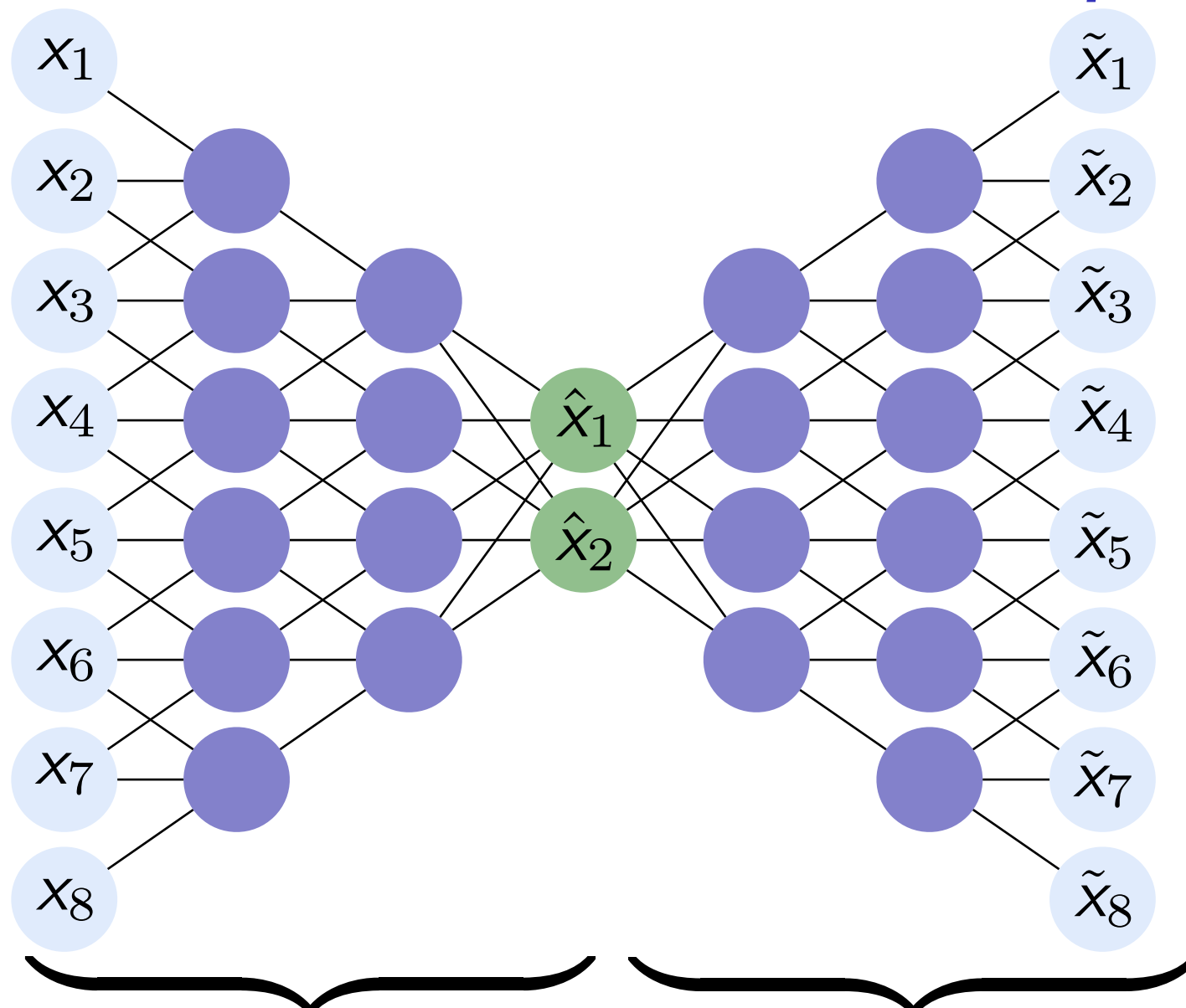
- + No problem-specific knowledge required
- + Use same snapshot data as POD

Deep convolutional autoencoders

$$\mathcal{S} := \{\mathbf{g}(\hat{\mathbf{x}}) \mid \hat{\mathbf{x}} \in \mathbb{R}^p\}$$

Deep autoencoders

Input layer *Code* *Output layer*

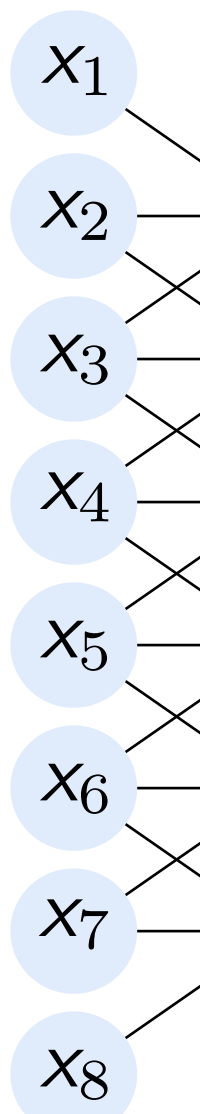


Encoder $\mathbf{h}_{\text{enc}}(\cdot; \theta_{\text{enc}})$ **Decoder** $\mathbf{h}_{\text{dec}}(\cdot; \theta_{\text{dec}})$

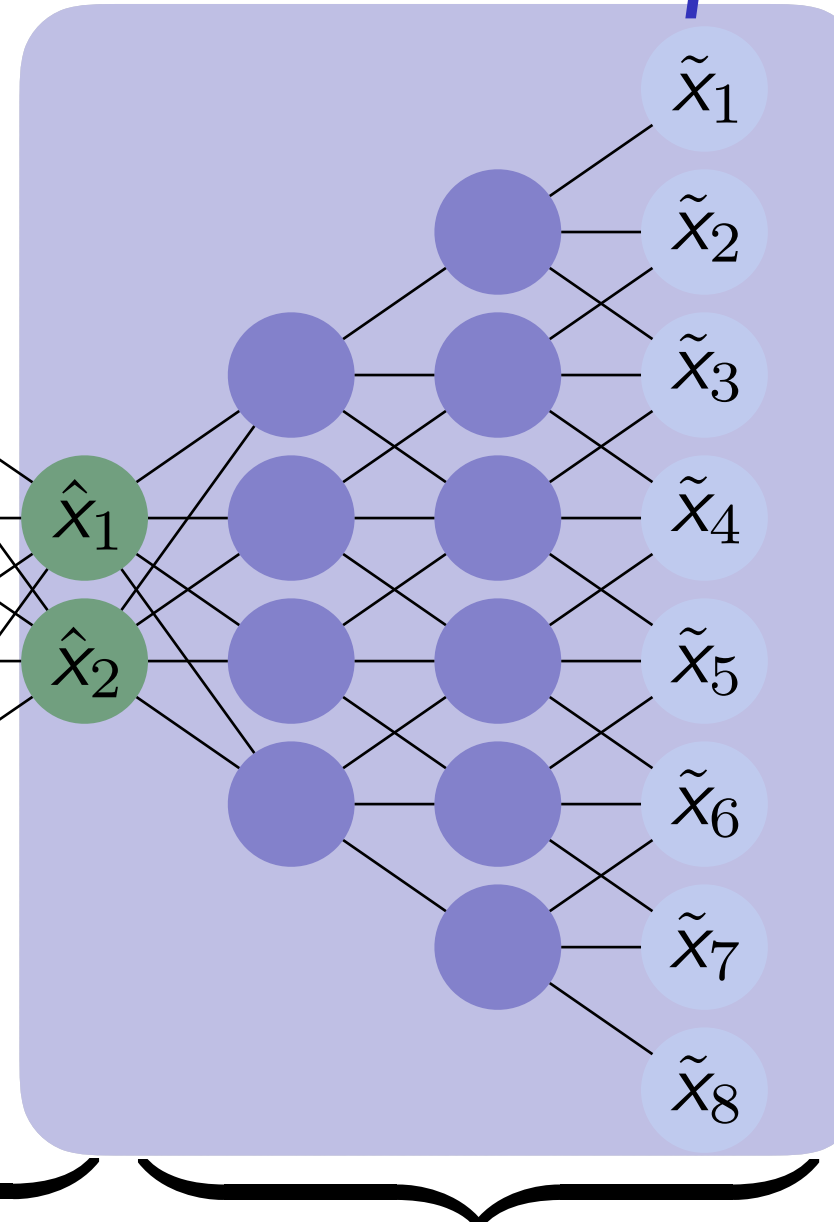
$$\tilde{\mathbf{x}} = \mathbf{h}_{\text{dec}}(\cdot; \theta_{\text{dec}}) \circ \mathbf{h}_{\text{enc}}(\mathbf{x}; \theta_{\text{enc}})$$

Deep autoencoders

Input layer



Code



Output layer

Encoder $\mathbf{h}_{\text{enc}}(\cdot; \theta_{\text{enc}})$ **Decoder** $\mathbf{h}_{\text{dec}}(\cdot; \theta_{\text{dec}})$

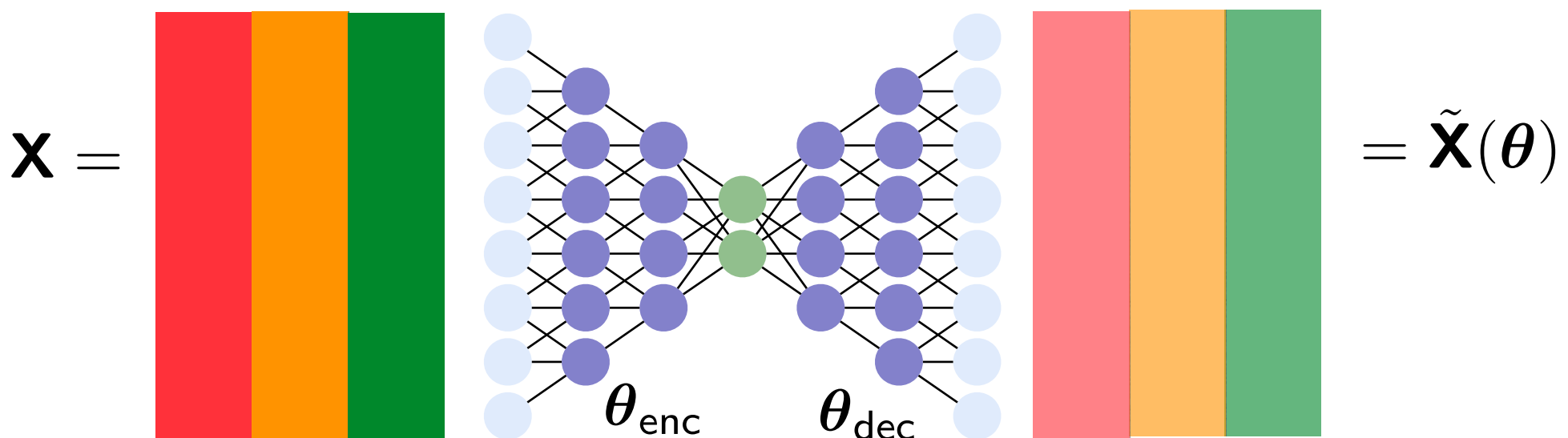
$$\tilde{\mathbf{x}} = \mathbf{h}_{\text{dec}}(\cdot; \theta_{\text{dec}}) \circ \mathbf{h}_{\text{enc}}(\mathbf{x}; \theta_{\text{enc}})$$

- + If $\tilde{\mathbf{x}} \approx \mathbf{x}$ for parameters θ_{dec}^* , $\mathbf{g} = \mathbf{h}_{\text{dec}}(\cdot; \theta_{\text{dec}}^*)$ produces an accurate manifold

1. *Training*: Solve ODE for $\mu \in \mathcal{D}_{\text{training}}$ and collect simulation data

2. *Machine learning*: Identify structure in data

3. *Reduction*: Reduce the cost of solving ODE for $\mu \in \mathcal{D}_{\text{query}} \setminus \mathcal{D}_{\text{training}}$

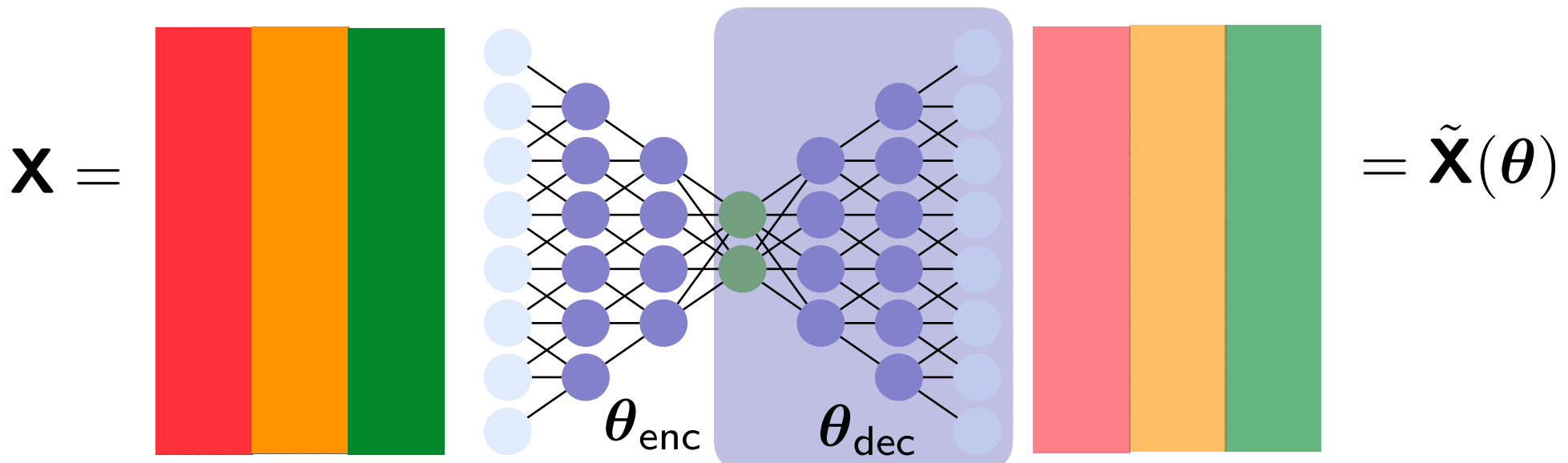


- Compute θ^* by approximately solving $\underset{\theta}{\text{minimize}} \|\mathbf{X} - \tilde{\mathbf{X}}(\theta)\|_F$

1. *Training*: Solve ODE for $\mu \in \mathcal{D}_{\text{training}}$ and collect simulation data

2. *Machine learning*: Identify structure in data

3. *Reduction*: Reduce the cost of solving ODE for $\mu \in \mathcal{D}_{\text{query}} \setminus \mathcal{D}_{\text{training}}$



- Compute θ^* by approximately solving $\underset{\theta}{\text{minimize}} \|\mathbf{X} - \tilde{\mathbf{X}}(\theta)\|_F$
- Define nonlinear trial manifold by setting $\mathbf{g} = \mathbf{h}_{\text{dec}}(\cdot; \theta_{\text{dec}}^*)$
- + Same snapshot data, no specialized problem knowledge

Numerical results

1D Burgers' equation

$$\frac{\partial w(x, t; \mu)}{\partial t} + \frac{\partial f(w(x, t; \mu))}{\partial x} = 0.02e^{\alpha x}$$

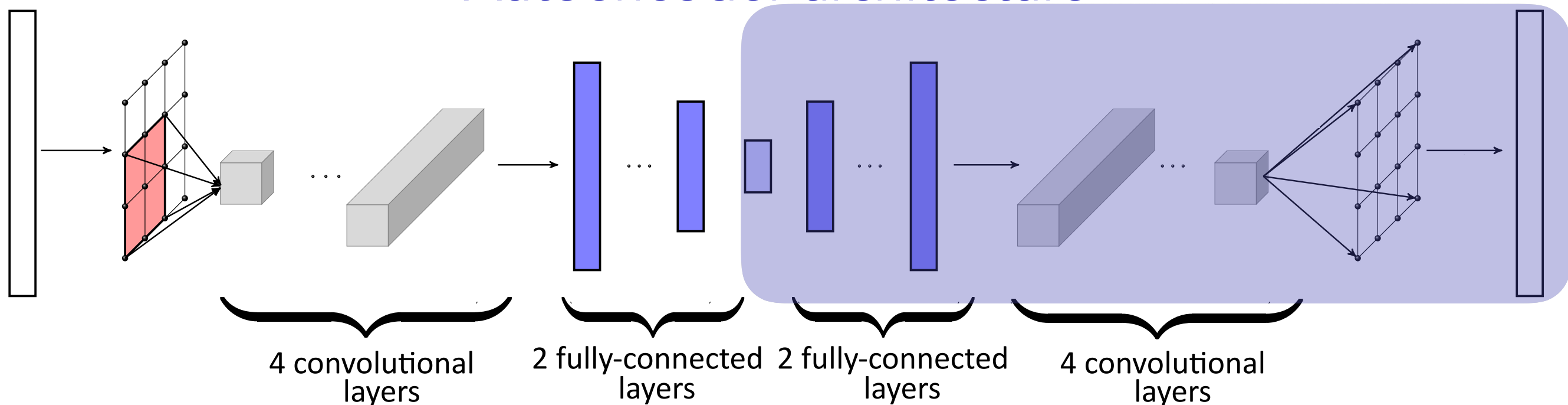
2D reacting flow

$$\begin{aligned} \frac{\partial \mathbf{w}(\vec{x}, t; \mu)}{\partial t} &= \nabla \cdot (\kappa \nabla \mathbf{w}(\vec{x}, t; \mu)) \\ &- \mathbf{v} \cdot \nabla \mathbf{w}(\vec{x}, t; \mu) + \mathbf{q}(\mathbf{w}(\vec{x}, t; \mu); \mu) \end{aligned}$$

- μ : α , inlet boundary condition
- *Spatial discretization*: finite volume
- *Time integrator*: backward Euler

- μ : two terms in reaction
- *Spatial discretization*: finite difference
- *Time integrator*: BDF2

Autoencoder architecture



Manifold interpretation: Burgers' equation

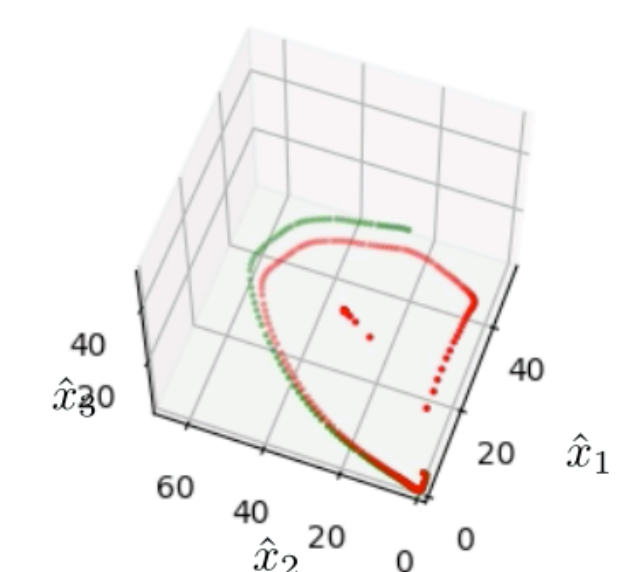
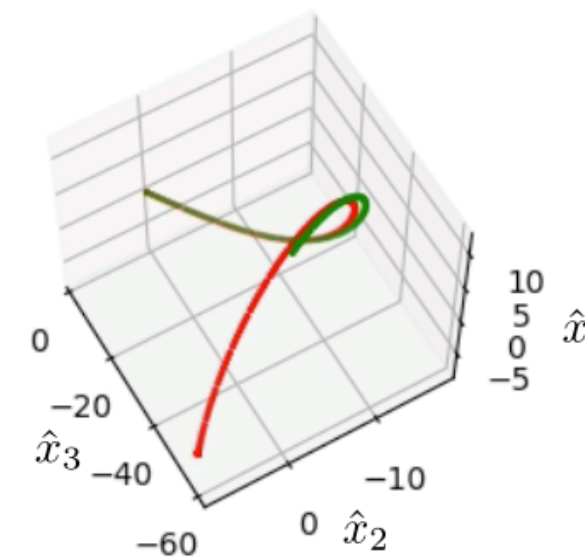
FOM

POD, $p=3$
projection

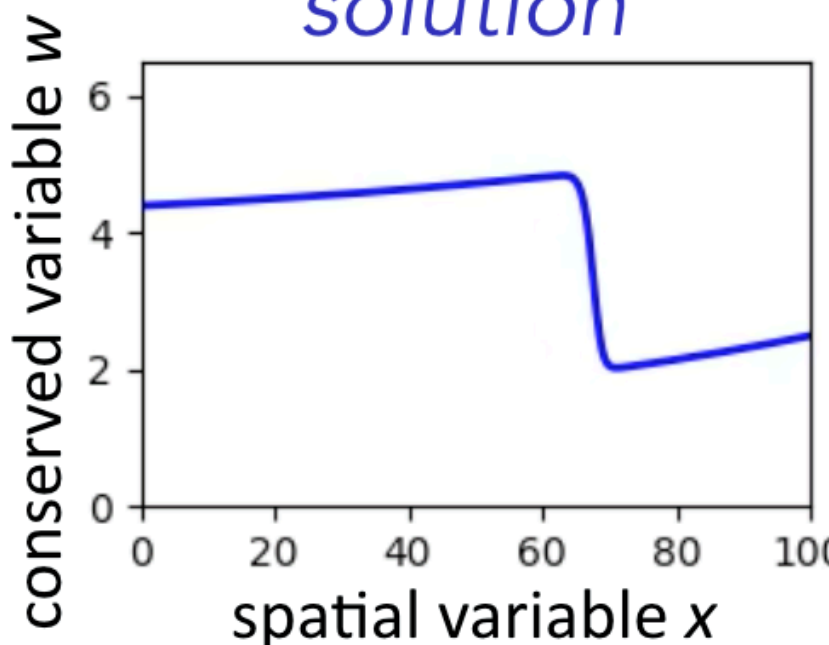
Autoencoder, $p=3$
projection

$t = 22.61, (\mu_1, \mu_2) = (4.39, 0.015)$

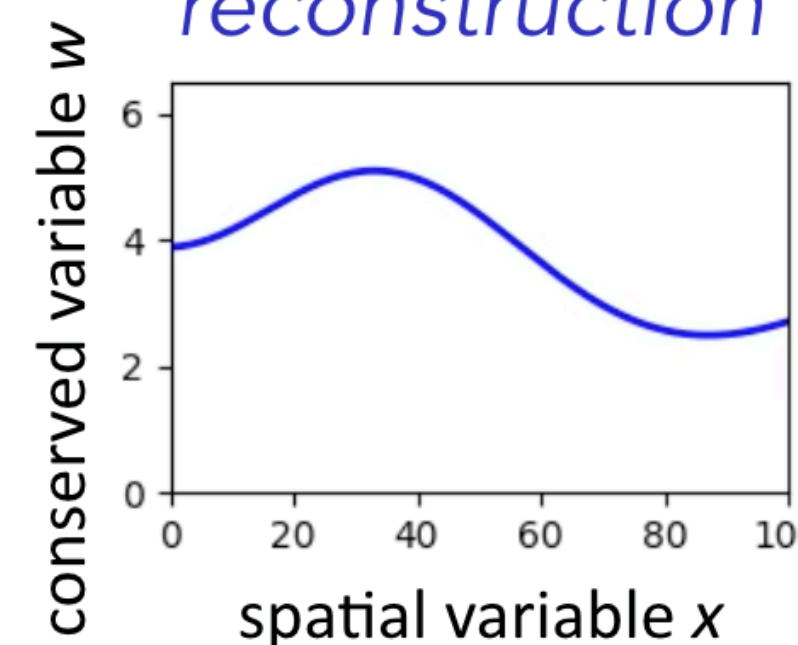
$t = 22.61, (\mu_1, \mu_2) = (4.39, 0.015)$



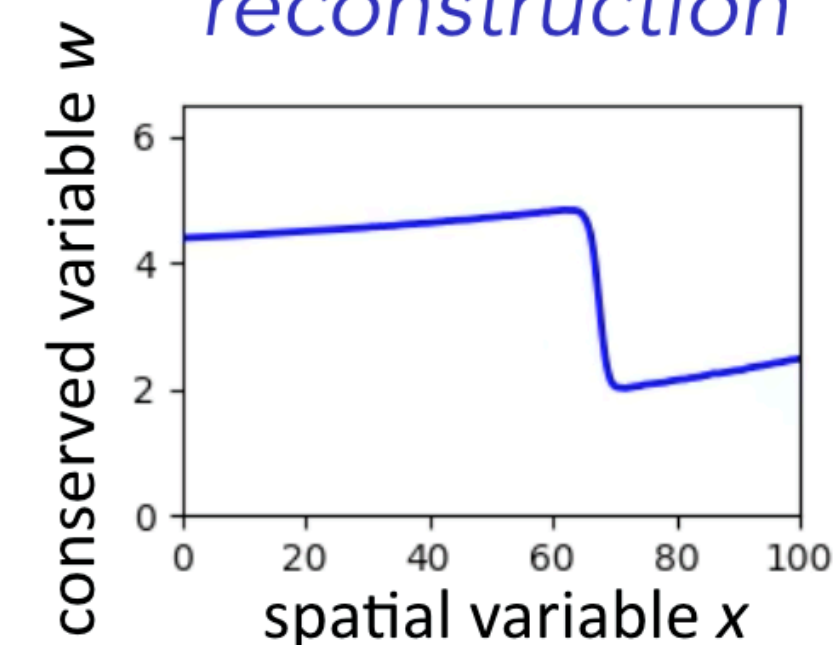
solution



reconstruction



reconstruction



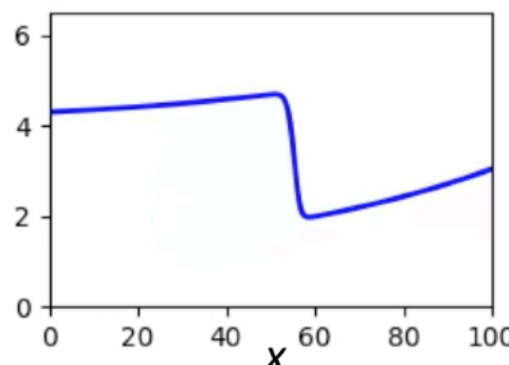
+ *Projection error onto 3-dimensional manifold nearly perfect*

Manifold LSPG outperforms optimal linear subspace

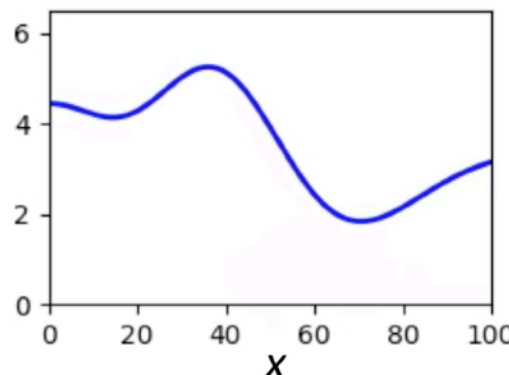
1D Burgers' equation

conserved variable

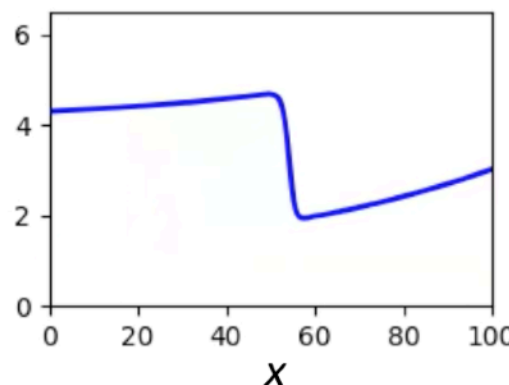
high-fidelity
model



POD-LSPG
 $p=5$



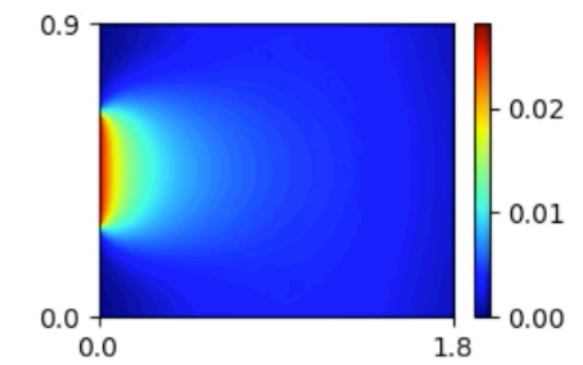
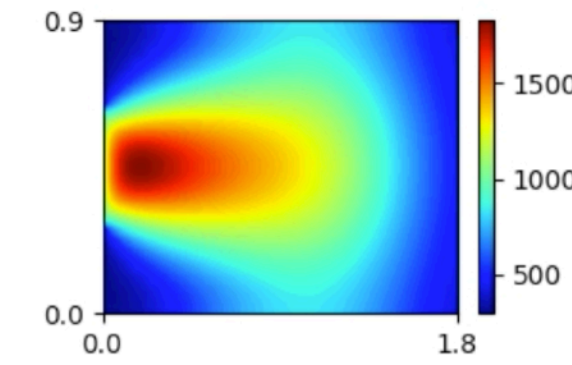
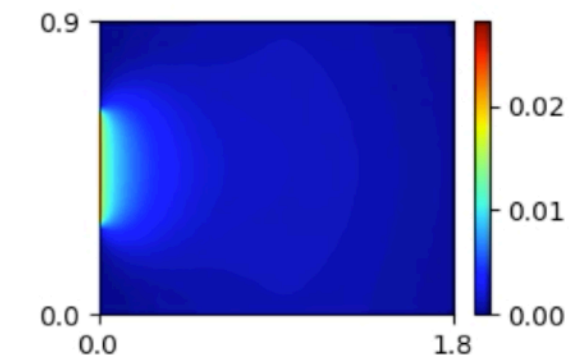
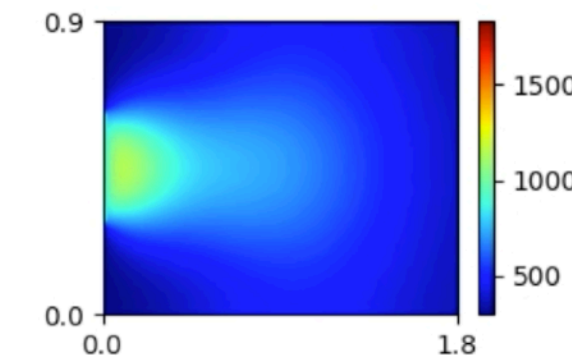
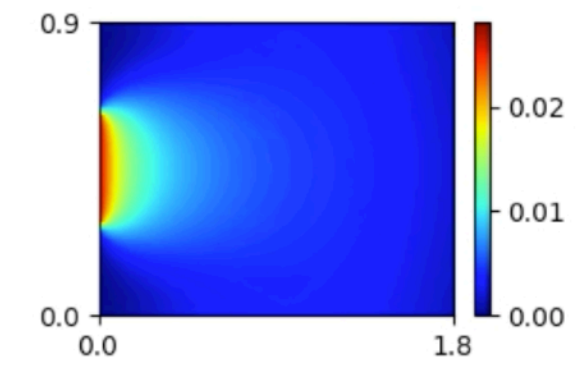
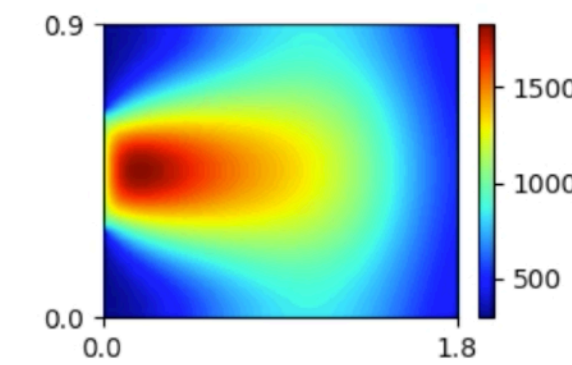
Manifold LSPG
 $p=5$



2D reacting flow

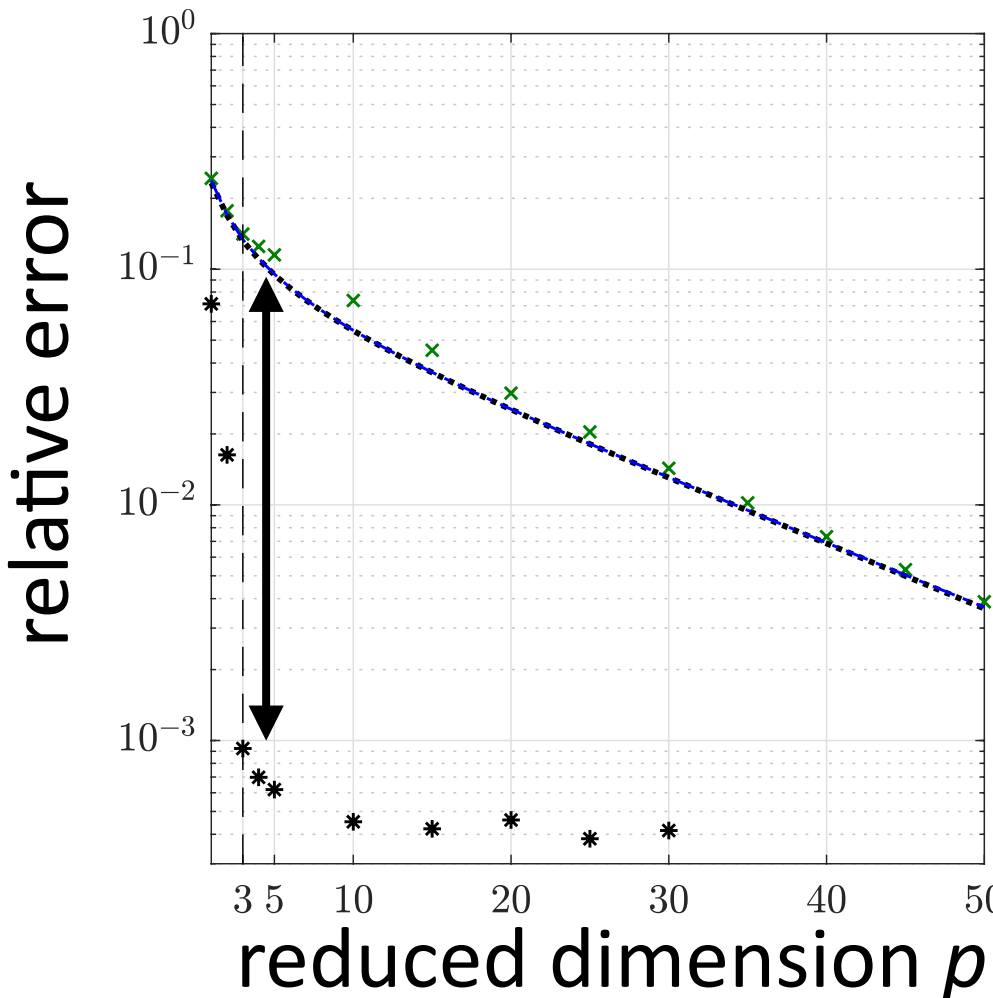
temperature

H_2 fraction

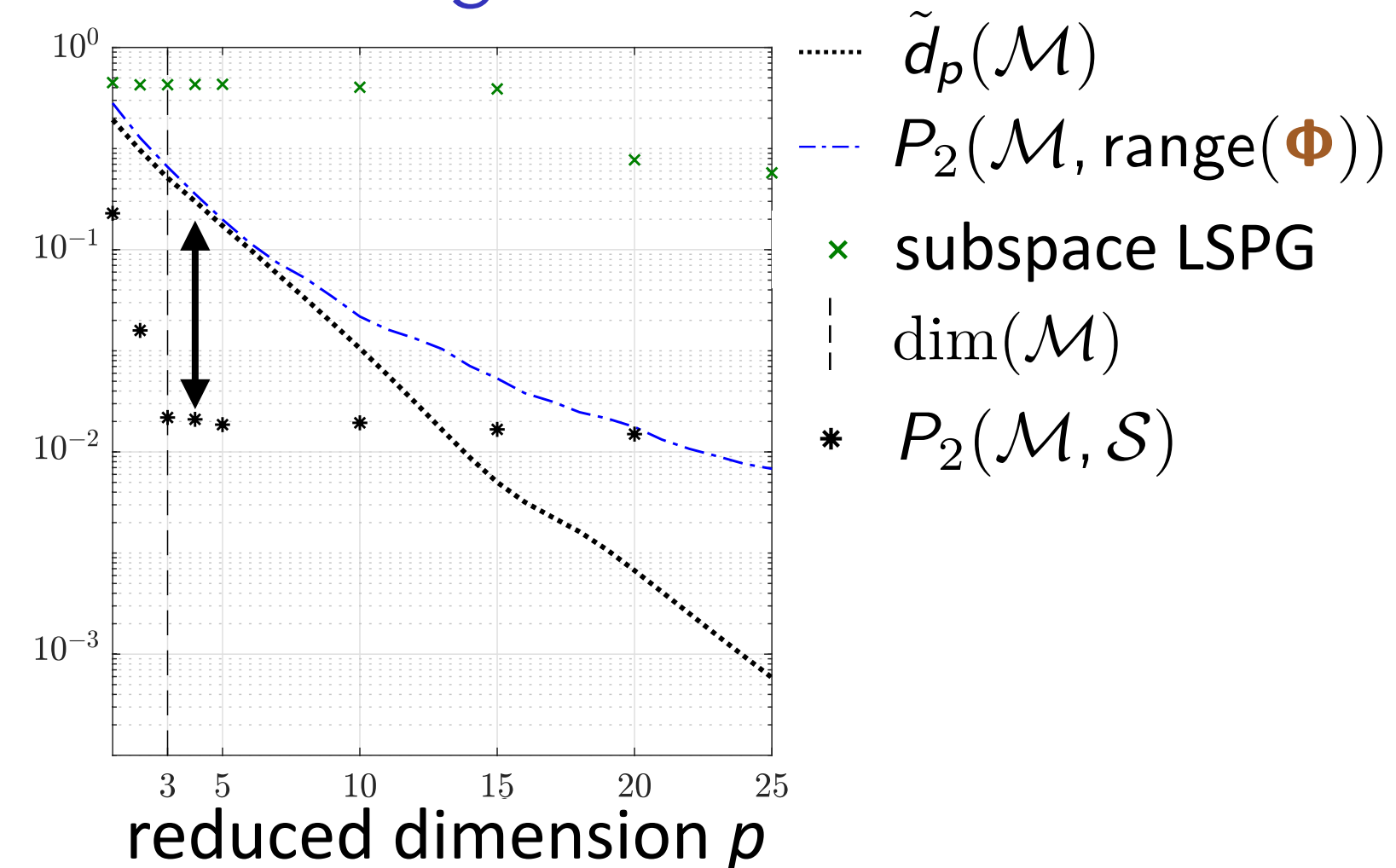


Method improves generalization performance

Burgers' equation



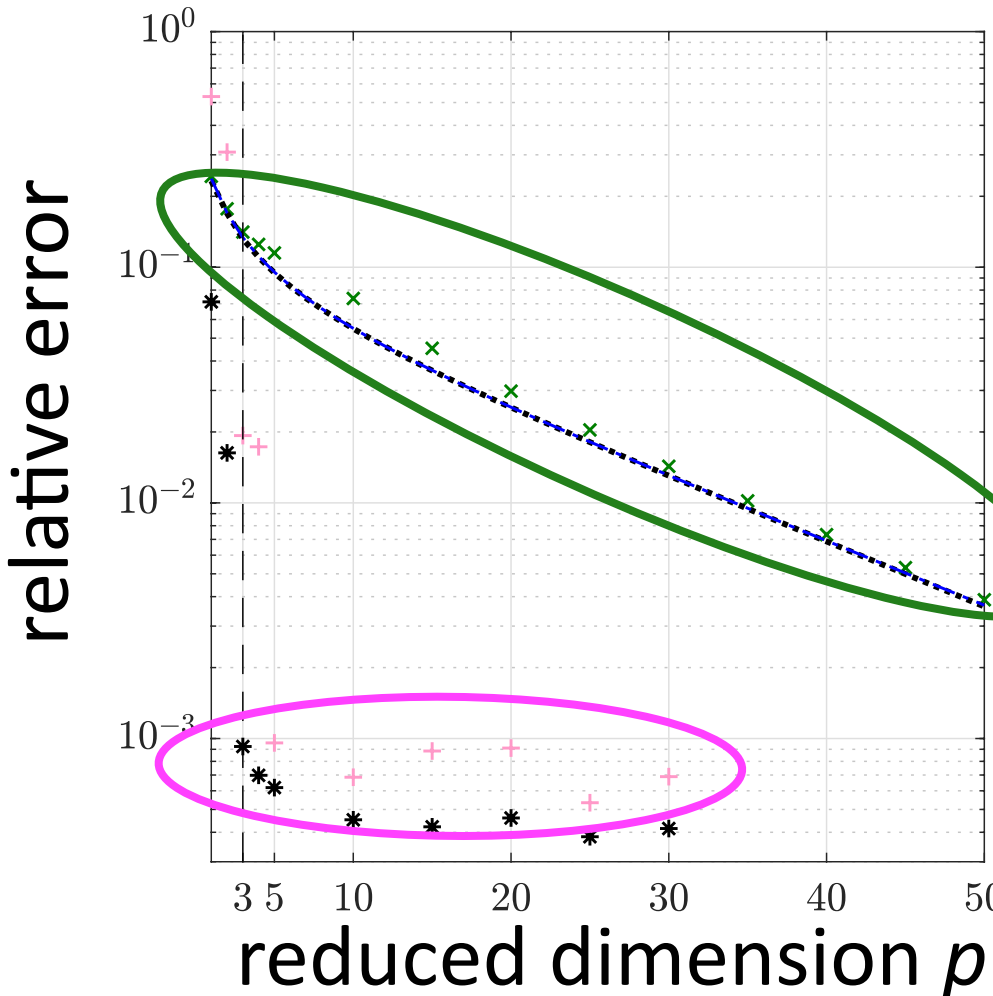
Reacting flow



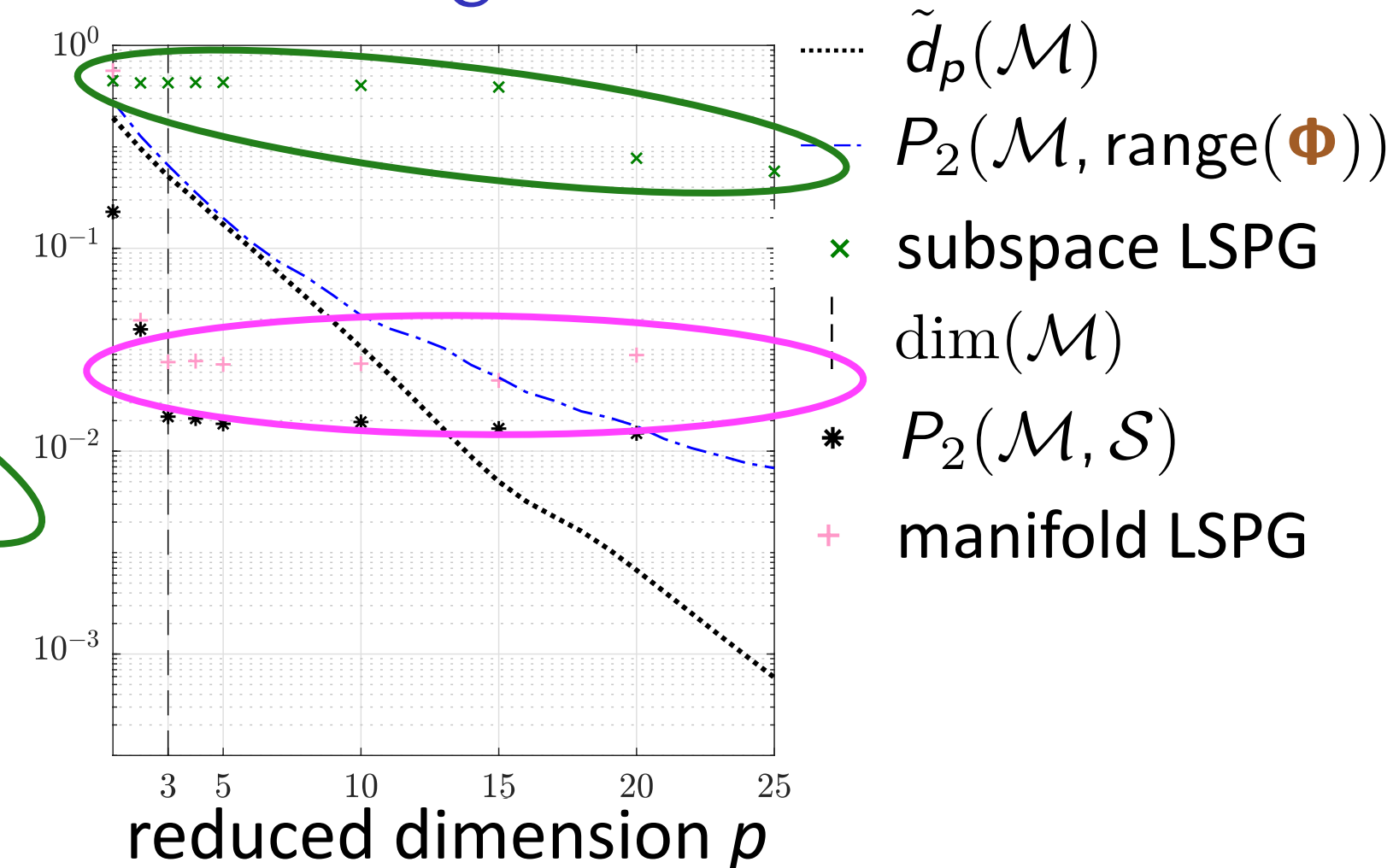
- + Autoencoder manifold **significantly better** than optimal linear subspace

Method improves generalization performance

Burgers' equation



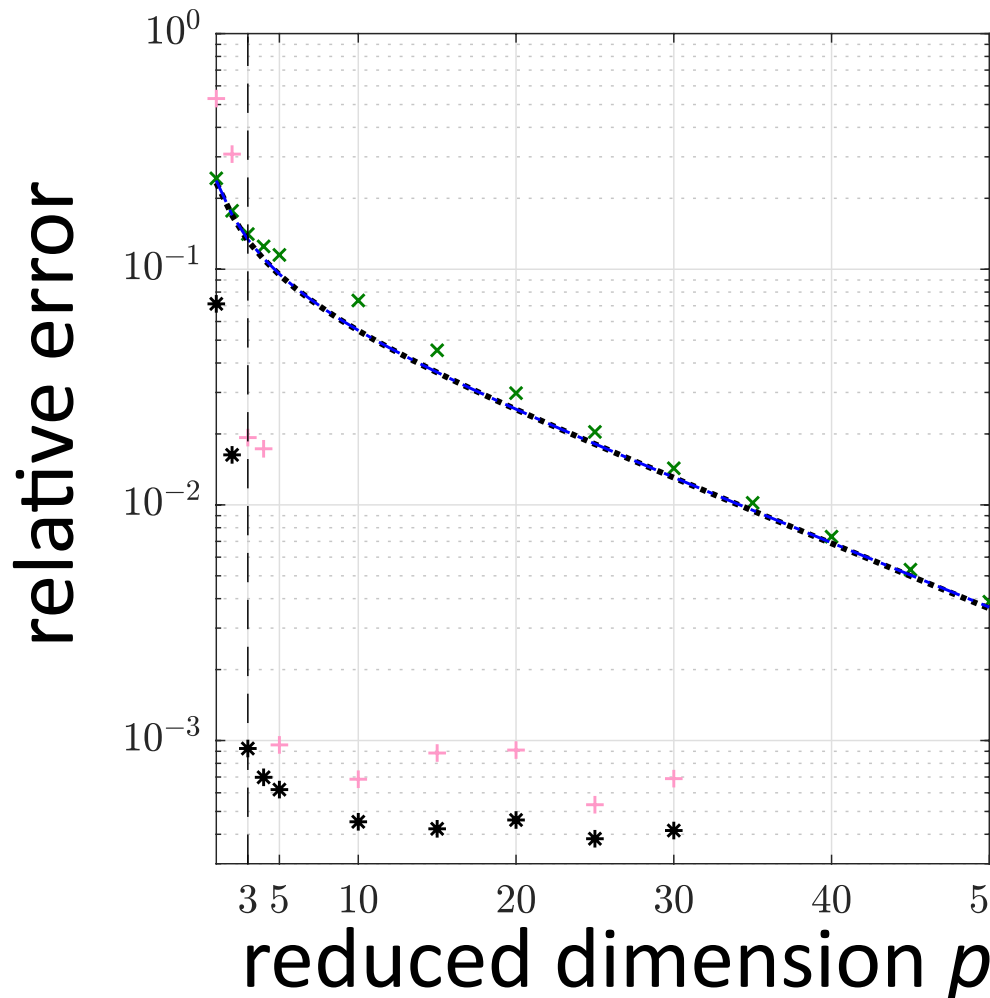
Reacting flow



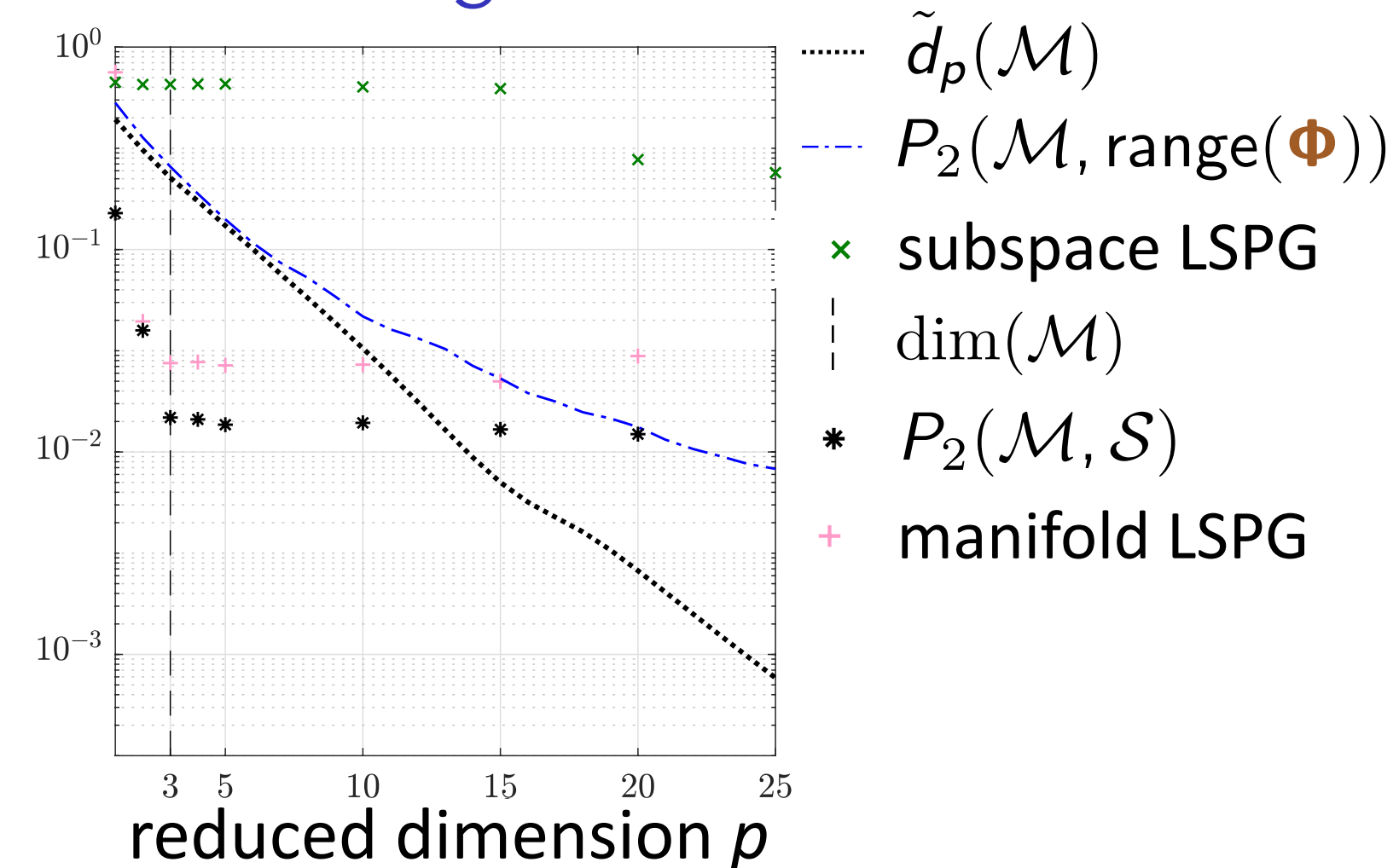
- + Autoencoder manifold **significantly better** than optimal linear subspace
- + Manifold LSPG orders-of-magnitude more accurate than subspace LSPG

Method improves generalization performance

Burgers' equation



Reacting flow

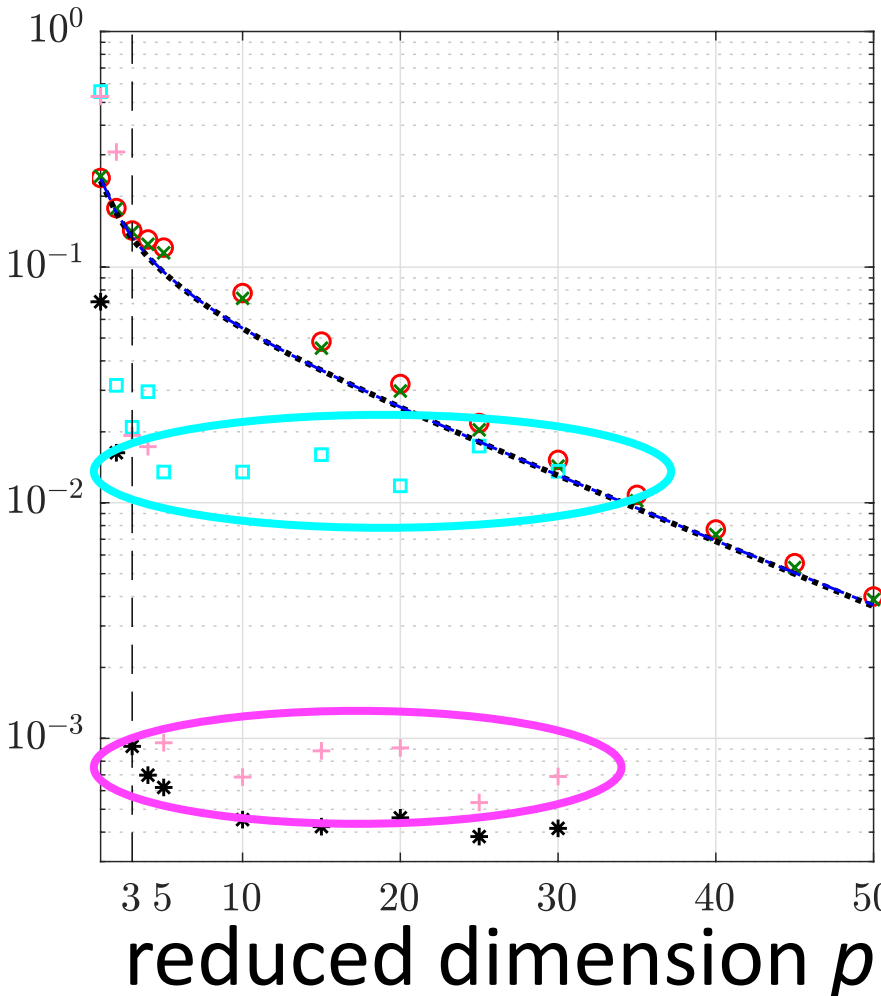


- + Autoencoder manifold **significantly better** than optimal linear subspace
- + **Manifold LSPG** orders-of-magnitude more accurate than **subspace LSPG**
- + Method **breaks Kolmogorov-width barrier**

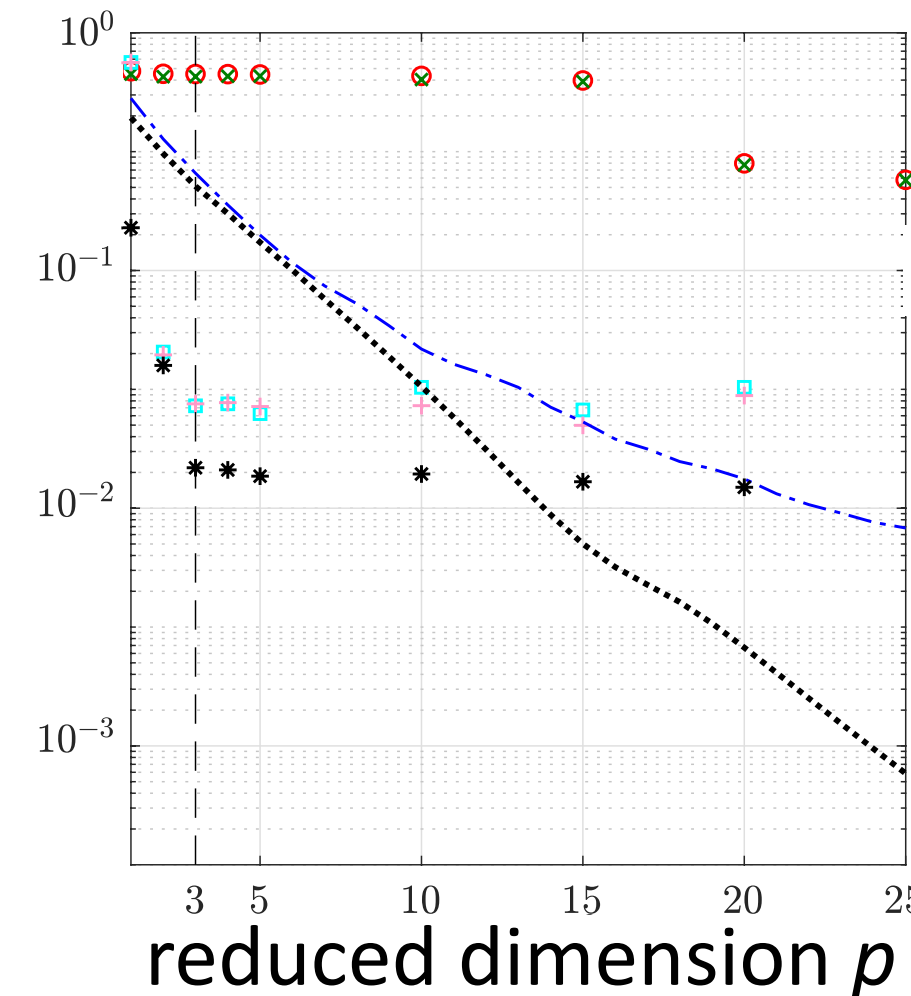
Method improves generalization performance

Burgers' equation

relative error



Reacting flow



- $\tilde{d}_p(\mathcal{M})$
- - - $P_2(\mathcal{M}, \text{range}(\Phi))$
- ✖ subspace LSPG
- $\dim(\mathcal{M})$
- * $P_2(\mathcal{M}, \mathcal{S})$
- + manifold LSPG
- subspace Galerkin
- manifold Galerkin

- + Autoencoder manifold **significantly better** than optimal linear subspace
- + Manifold LSPG orders-of-magnitude more accurate than subspace LSPG
- + Method **breaks Kolmogorov-width barrier**
- + Manifold LSPG outperforms manifold Galerkin on 1D Burgers' equation

Manifold Galerkin

$$\frac{d\hat{\mathbf{x}}}{dt} = \underset{\hat{\mathbf{v}} \in \mathbb{R}^n}{\operatorname{argmin}} \| \mathbf{r}(\nabla \mathbf{g}(\hat{\mathbf{x}})\hat{\mathbf{v}}, \mathbf{g}(\hat{\mathbf{x}}); t) \|_2$$

Manifold LSPG

$$\hat{\mathbf{x}}^n = \underset{\hat{\mathbf{v}} \in \mathbb{R}^p}{\operatorname{argmin}} \| \mathbf{r}^n(\mathbf{g}(\hat{\mathbf{v}})) \|_2$$

Interpretation

- Predictions directly integrate deep learning with computational physics

Manifold Galerkin

$$\frac{d\hat{\mathbf{x}}}{dt} = \underset{\hat{\mathbf{v}} \in \mathbb{R}^n}{\operatorname{argmin}} \| \mathbf{r}(\nabla \mathbf{g}(\hat{\mathbf{x}})\hat{\mathbf{v}}, \mathbf{g}(\hat{\mathbf{x}}); t) \|_2$$

Manifold LSPG

$$\hat{\mathbf{x}}^n = \underset{\hat{\mathbf{v}} \in \mathbb{R}^p}{\operatorname{argmin}} \| \mathbf{r}^n(\mathbf{g}(\hat{\mathbf{v}})) \|_2$$

Interpretation

- Predictions directly integrate **deep learning** with **computational physics**
- Latent dynamics model via *projection of governing equations*
- Nearly all existing latent dynamics models are purely *data driven*

[Böhmer et al., 2015; Goroshin et al., 2015; Watter et al., 2015; Karl et al., 2017; Takeishi et al., 2017; Banjamali et al., 2018; Lesort et al., 2018; Lusch et al., 2018; Morton et al., 2018 Otto and Rowley, 2019]

Manifold Galerkin

$$\frac{d\hat{\mathbf{x}}}{dt} = \underset{\hat{\mathbf{v}} \in \mathbb{R}^n}{\operatorname{argmin}} \| \mathbf{r}(\nabla \mathbf{g}(\hat{\mathbf{x}})\hat{\mathbf{v}}, \mathbf{g}(\hat{\mathbf{x}}); t) \|_2$$

Manifold LSPG

$$\hat{\mathbf{x}}^n = \underset{\hat{\mathbf{v}} \in \mathbb{R}^p}{\operatorname{argmin}} \| \mathbf{r}^n(\mathbf{g}(\hat{\mathbf{v}})) \|_2$$

Interpretation

- Predictions directly integrate **deep learning** with **computational physics**
- Latent dynamics model via *projection of governing equations*
- Nearly all existing latent dynamics models are purely *data driven*

[Böhmer et al., 2015; Goroshin et al., 2015; Watter et al., 2015; Karl et al., 2017; Takeishi et al., 2017; Banjamali et al., 2018; Lesort et al., 2018; Lusch et al., 2018; Morton et al., 2018 Otto and Rowley, 2019]

Gradient computation

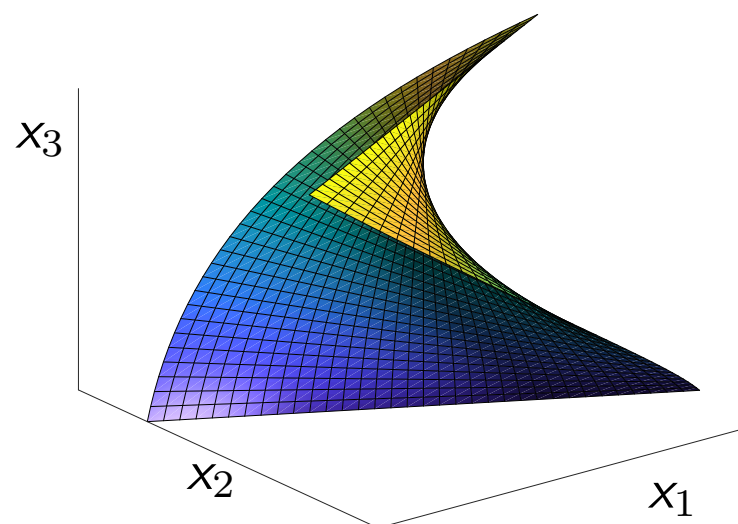
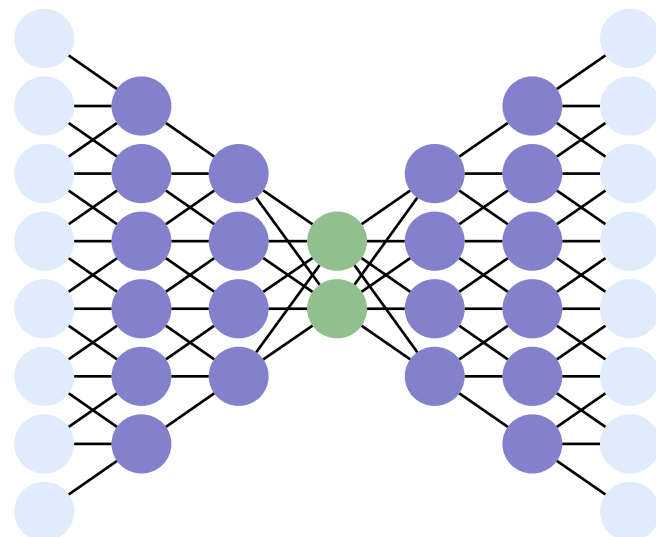
- Backpropagation used to compute decoder Jacobian $\nabla \mathbf{g}(\hat{\mathbf{x}})$
- Quasi-Newton solvers directly call TensorFlow

Forward-compatible extensions

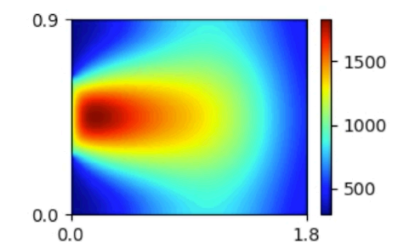
- *Hyper-reduction*: convolutional layers preserve sparsity
- *Structure preservation*: equality constraints enforcing conservation

Questions?

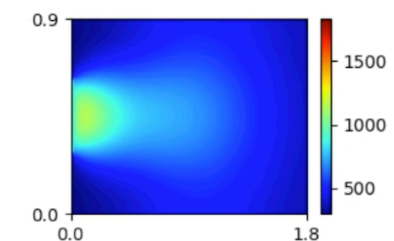
Reference: Lee and C. "Model reduction of dynamical systems on nonlinear manifolds using deep convolutional autoencoders," arXiv e-Print, 1812.08373 (2018).



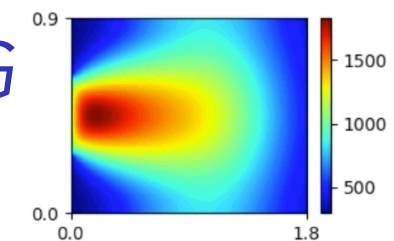
high-fidelity
model



POD-LSPG
 $p=5$

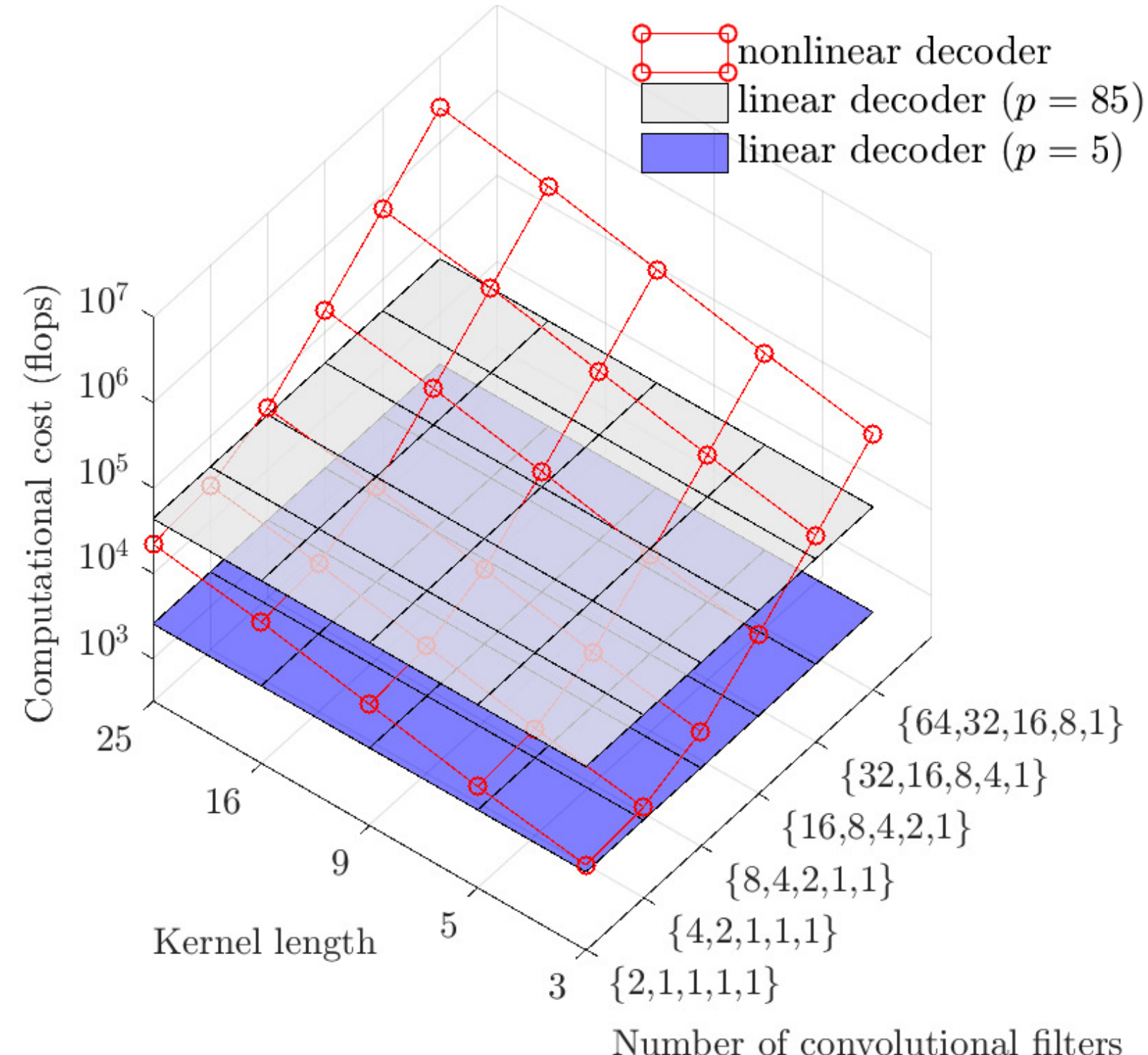


Manifold LSPG
 $p=5$



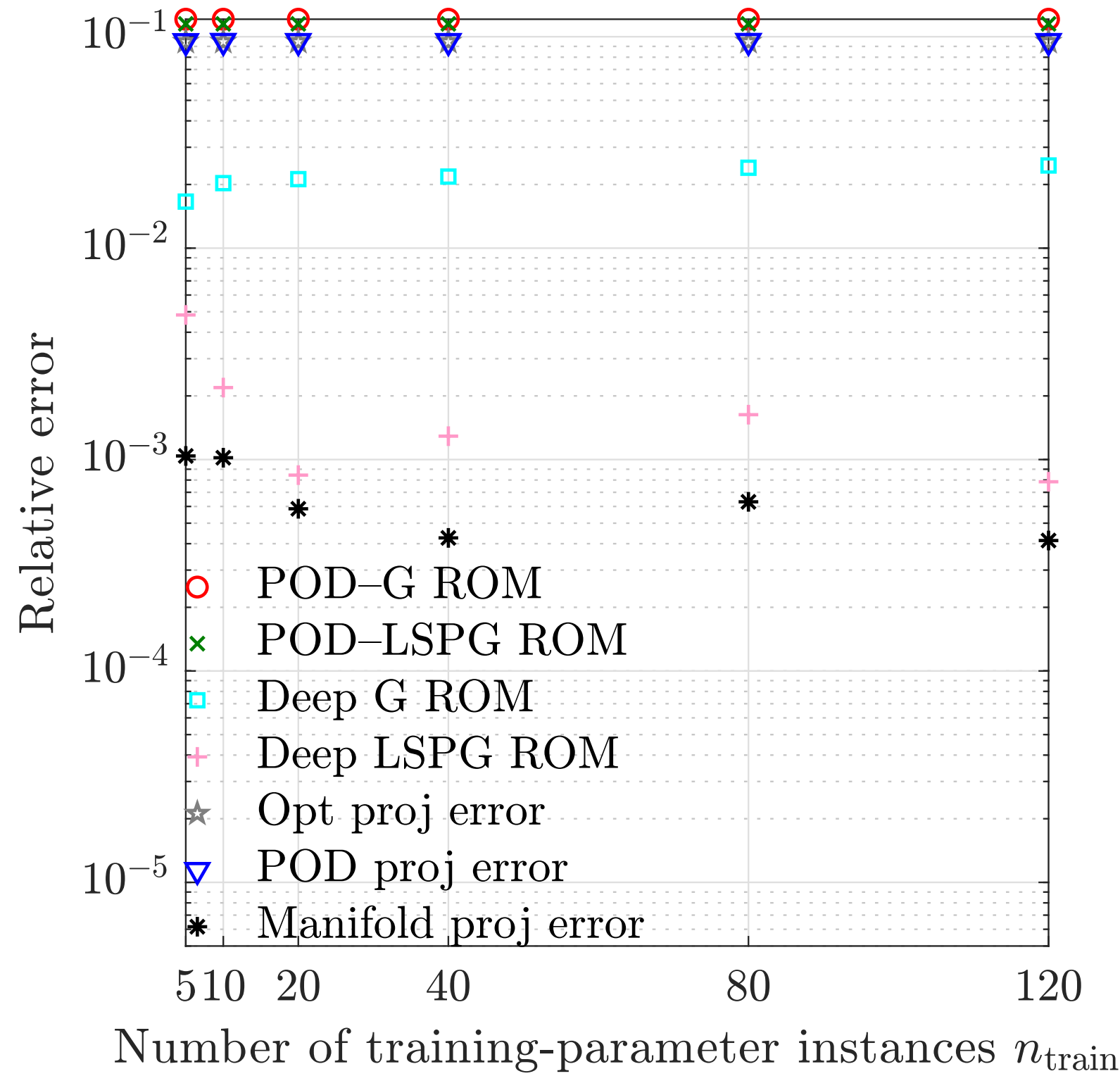
Sandia National Laboratories is a multimission laboratory managed and operated by National Technology and Engineering Solutions of Sandia, LLC, a wholly owned subsidiary of Honeywell International, Inc., for the U.S. Department of Energy's National Nuclear Security Administration under contract DE-NA-0003525. Lawrence Livermore National Laboratory is operated by Lawrence Livermore National Security, LLC, for the U.S. Department of Energy, National Nuclear Security Administration under Contract DE-AC52-07NA27344.

Computational cost



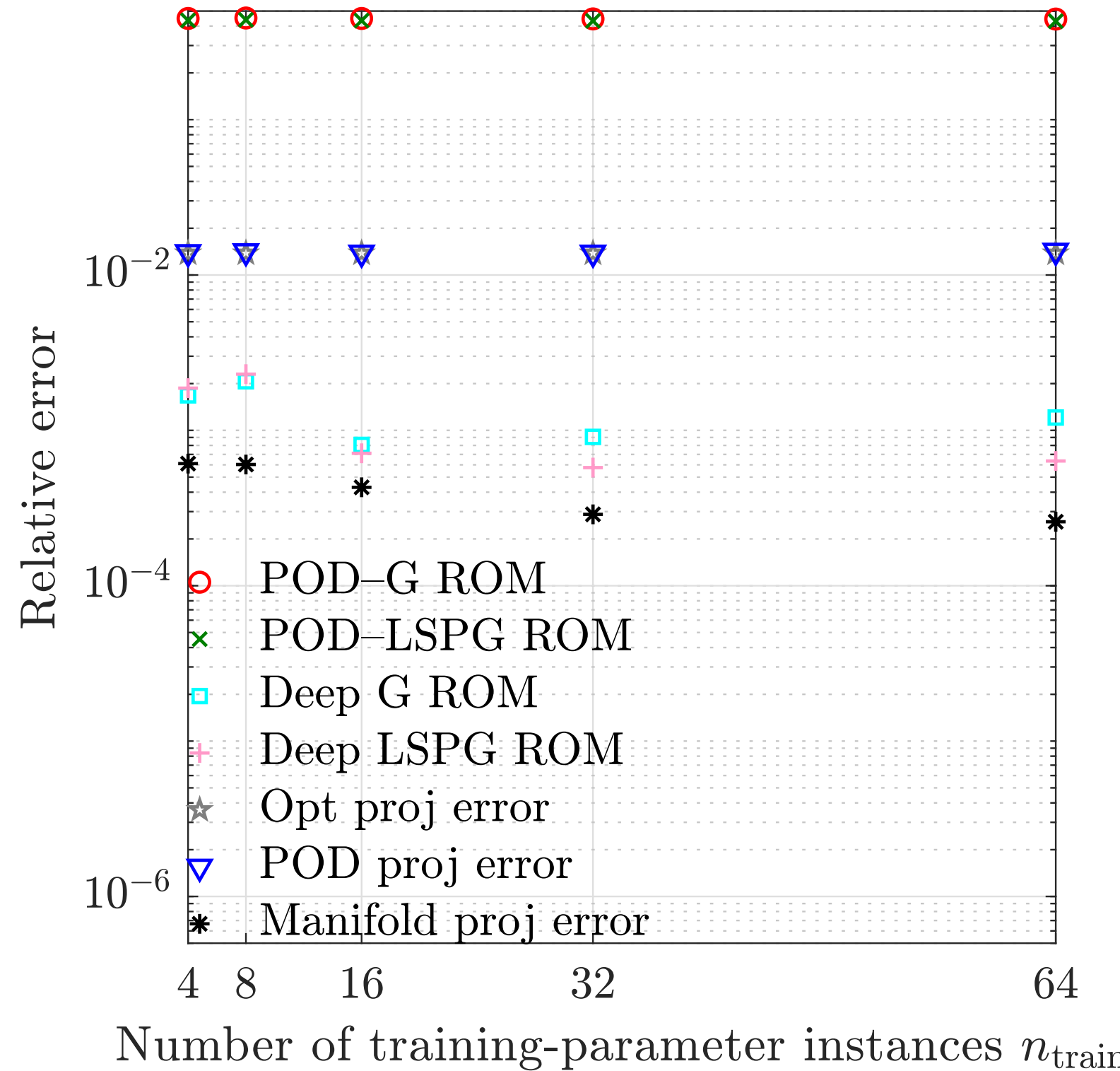
- Architecture dictates computational cost of nonlinear decoder
- + Can achieve costs **comparable to linear decoders**

Dependence on training data: Burgers'



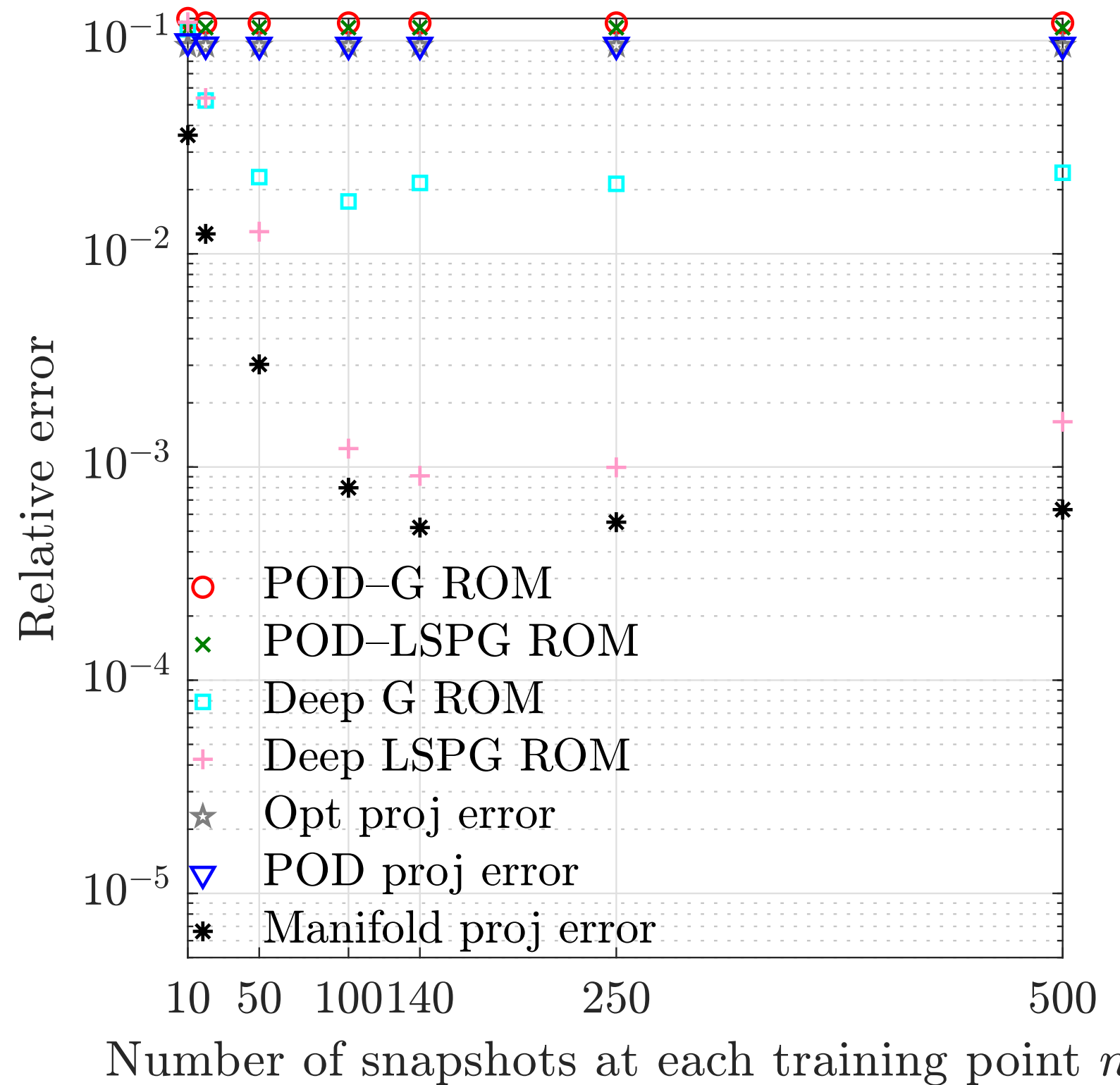
+ Manifold LSPG: <1% errors with only 5 training points

Dependence on training data: Chemically



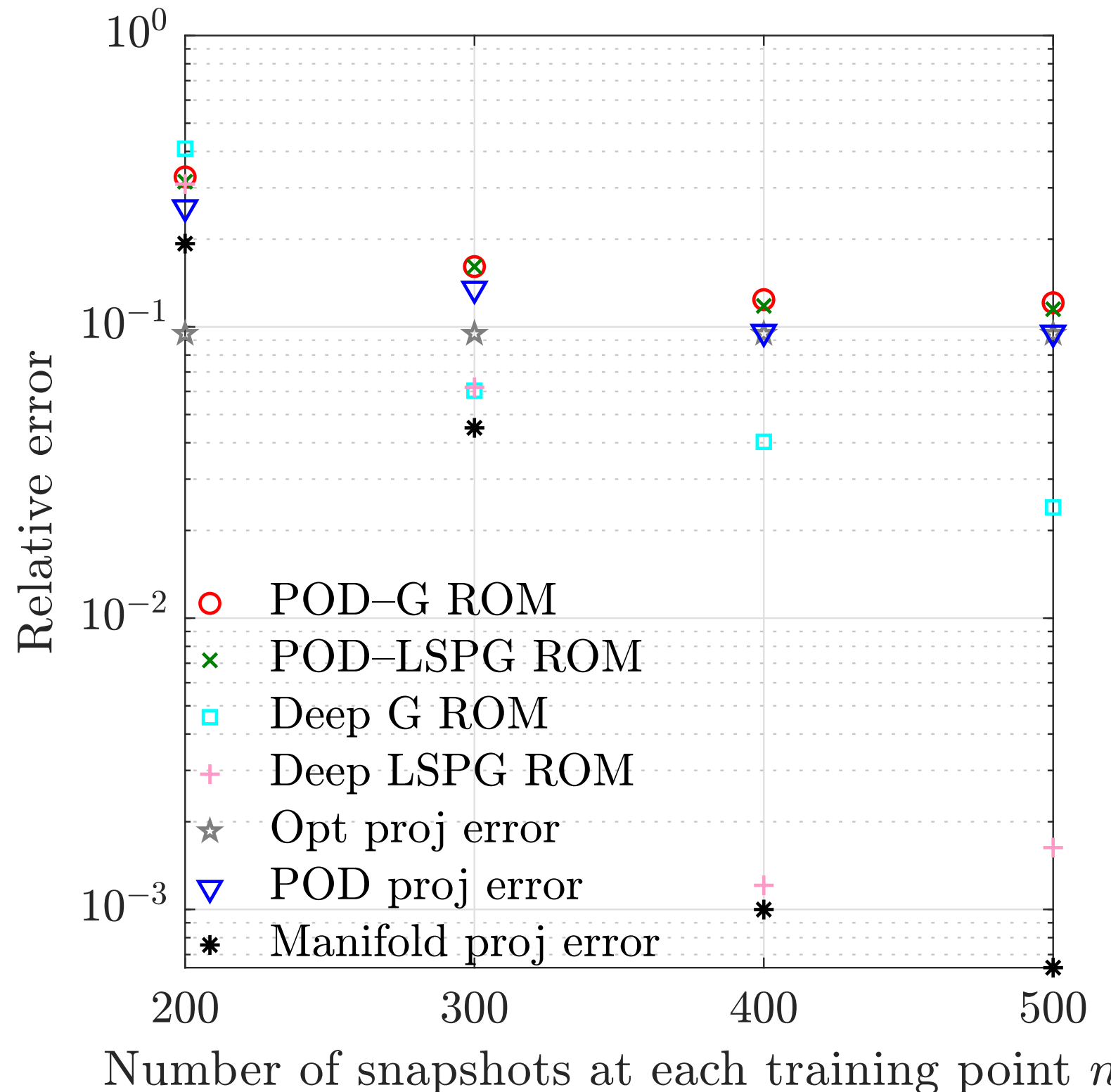
+ Manifold LSPG and Galerkin: <1% errors with only 4 training points

Time interpolation: Burgers' equation



+ Manifold LSPG can interpolate well with at least 20% snapshots

Time extrapolation: Burgers' equation



+ Manifold LSPG can extrapolate well with at least 80% snapshots